

CANCER

ERK signaling mediates resistance to immunomodulatory drugs in the bone marrow microenvironment

Jiye Liu^{1†}, Teru Hideshima^{1†}, Lijie Xing^{1,2}, Su Wang^{3‡}, Wenrong Zhou⁴, Mehmet K. Samur^{1,5}, Tomasz Sewastianik^{6,7}, Daisuke Ogiya^{1§}, Gang An⁸, Shaobing Gao⁹, Li Yang¹⁰, Tong Ji¹¹, Giada Bianchi¹², Kenneth Wen¹, Yu-Tzu Tai¹, Nikhil Munshi¹, Paul Richardson¹, Ruben Carrasco^{6,13}, Yong Cang¹⁴, Kenneth C. Anderson^{1*}

Immunomodulatory drugs (IMiDs) have markedly improved patient outcome in multiple myeloma (MM); however, resistance to IMiDs commonly underlies relapse of disease. Here, we identify that tumor necrosis factor (TNF) receptor-associated factor 2 (TRAF2) knockdown (KD)/knockout (KO) in MM cells mediates IMiD resistance via activation of noncanonical nuclear factor κ B (NF- κ B) and extracellular signal-regulated kinase (ERK) signaling. Within MM bone marrow (BM) stromal cell supernatants, TNF- α induces proteasomal degradation of TRAF2, noncanonical NF- κ B, and downstream ERK signaling in MM cells, whereas interleukin-6 directly triggers ERK activation. RNA sequencing of MM patient samples shows nearly universal ERK pathway activation at relapse on lenalidomide maintenance therapy, confirming its clinical relevance. Combination MEK inhibitor treatment restores IMiD sensitivity of TRAF2 KO cells both in vitro and in vivo. Our studies provide the framework for clinical trials of MEK inhibitors to overcome IMiD resistance in the BM microenvironment and improve patient outcome in MM.

INTRODUCTION

Multiple myeloma (MM) is characterized by the infiltration of abnormal plasma cells in the bone marrow (BM) and monoclonal protein in serum and/or urine, associated with hypercalcemia, renal dysfunction, anemia, and bone disease (1). The development of high-dose therapy and autologous stem cell transplantation (2, 3) and, more recently, of novel agents including proteasome inhibitors (4), histone deacetylase inhibitor (5, 6), immunomodulatory drugs (IMiDs) (7–9), and monoclonal antibodies (Abs) (10–12), has transformed therapy and markedly improved patient outcome.

The IMiD thalidomide (Thal) was banned because of its teratogenicity when prescribed to treat morning sickness of pregnant women 50 years ago (13). However, Thal and its analogs lenalidomide (Len) and pomalidomide (Pom), initially used empirically predicated upon their antiangiogenic activity (14), have demonstrated remarkable clinical efficacy in MM and other B cell malignancies (15). Our early studies showed that IMiDs trigger direct MM cytotoxicity via activation of caspase-8-mediated extrinsic apoptotic pathway, as well as enhancing immune effector antitumor responses while inhibiting T regulatory cells (16–19). Multiple groups have subsequently reported that IMiDs directly bind cereblon (CRBN), a substrate adaptor of Cullin4 RING Ligase (CRL4) (20, 21) and activate CRL4^{CRBN} ligase, thereby selectively targeting two B cell transcription factors IKAROS Family Zinc Finger 1 (IKZF1) and IKAROS Family Zinc Finger 3 (IKZF3) for ubiquitination and proteasomal degradation (22, 23). We have also shown that IMiDs directly bind and inhibit TP53-regulating kinase activity in MM cells, followed by MM cell growth inhibition (24). IMiDs trigger additive or synergistic anti-MM activity when combined with proteasome inhibitors and monoclonal Abs in pre-clinical models (25, 26) and are now used in combinations to treat both newly diagnosed and relapsed MM. However, development of resistance to IMiDs commonly underlies relapse of disease.

To delineate mechanisms of IMiD resistance, the majority of previous studies have focused on CRBN. The expression level of CRBN, CRBN-binding proteins, and CRL4^{CRBN} ligase have been associated with IMiD sensitivity (27–30). For example, our prior studies used CRISPR-Cas9 screening to identify signalosome genes regulating expression of CRBN and IMiD sensitivity (31). Although down-regulation or mutations in CRBN have been associated with IMiD resistance (32, 33), MM cells can manifest resistance without CRBN dysfunction (34), indicating potential alternative mechanisms of IMiD resistance. We and others have also shown that MM cell adhesion to extracellular matrix proteins and accessory cells triggers

¹Jerome Lipper Multiple Myeloma Center, Department of Medical Oncology, Dana-Farber Cancer Institute, Harvard Medical School, Boston, MA 02215, USA. ²Department of Hematology, Shandong Provincial Hospital Affiliated to Shandong First Medical University, Jinan, Shandong 250021, China. ³Department of Biomedical Informatics, Harvard Medical School, Boston, MA 02115, USA. ⁴Oncology and Immunology Unit, Research Service Division, WuXi AppTec (Shanghai) Co., Ltd., Shanghai 200131, China. ⁵Department of Biostatistics and Computational Biology, Harvard T.H. Chan School of Public Health, Boston, MA 02115, USA. ⁶Department of Oncologic Pathology, Dana-Farber Cancer Institute, Harvard Medical School, Boston, MA 02215, USA. ⁷Department of Experimental Hematology, Institute of Hematology and Transfusion Medicine, Warsaw 02776, Poland. ⁸State Key Laboratory of Experimental Hematology, Institute of Hematology and Blood Diseases Hospital, Chinese Academy of Medical Science and Peking Union Medical College, Tianjin 300020, China. ⁹The Affiliated Cancer Hospital of Zhengzhou University, Zhengzhou 450008, China. ¹⁰Multiple Myeloma Treatment Center and Bone Marrow Transplantation Center, The First Affiliated Hospital, Zhejiang University School of Medicine, Hangzhou 310003, China. ¹¹Department of General Surgery, Sir Run Run Shaw Hospital, Zhejiang University School of Medicine, Hangzhou 310020, China. ¹²Division of Hematology, Department of Internal Medicine, Brigham and Women's Hospital, Harvard Medical School, Boston, MA 02115, USA. ¹³Department of Pathology, Brigham and Women's Hospital, Harvard Medical School, Boston, MA 02115, USA. ¹⁴School of Life Science and Technology, ShanghaiTech University, Shanghai 201210, China.

*Corresponding author. Email: kenneth_anderson@dfci.harvard.edu

†These authors contributed equally to this work.

‡Present address: Vertex Pharmaceuticals, 50 Northern Avenue, Boston, MA 02210, USA.

§Present address: Department of Hematology and Oncology, Tokai University School of Medicine, Isehara 259-1193, Japan.

cell adhesion-mediated drug resistance to conventional therapeutic agents (35, 36). Moreover, secretion of soluble factors [i.e., tumor necrosis factor- α (TNF- α) and interleukin-6 (IL-6)] from cellular components [i.e., BM stromal cells (BMSCs), osteoclasts, and vascular endothelial cells] activates intracellular signaling pathways including nuclear factor κ B (NF- κ B), Raf-mitogen-activated protein kinase (MAPK) kinase (MEK)-extracellular signal-regulated kinase (ERK), Janus kinase-signal transducer and activator of transcription, and phosphatidylinositol 3-kinase-Akt, thereby promoting migration, proliferation, survival, and drug resistance of MM cells (37). Resistance to dexamethasone-induced MM cell apoptosis, for example, is completely abrogated by coculture with BMSCs, IL-6, or insulin-like growth factor 1 α (IGF-1 α). To date, however, the molecular mechanisms mediating IMiD resistance have not been fully delineated.

In this study, we used our in vitro and in vivo preclinical model systems of MM in the BM milieu to delineate molecular mechanisms underlying sensitivity to IMiDs. Genome-wide CRISPR-Cas9 knockout (KO) screening identified *TRAF2*, a member of TNF receptor-associated factor (TRAF) protein family, to regulate IMiD sensitivity. We show that *TRAF2* KO-induced IMiD resistance is mediated via activation of noncanonical NF- κ B and downstream MEK-ERK signaling, independent of CRBN-IKZF1/3 axis. Within MM BMSC supernatants (SC-sup), TNF- α induces proteasomal degradation of TRAF2, followed by noncanonical NF- κ B and downstream ERK signaling, whereas IL-6 directly triggers ERK activation. Combination MEK inhibitor treatment restores IMiD sensitivity of *TRAF2* KO cells with high phosphorylated ERK (p-ERK) both in vitro in the presence of SC-sup and in vivo in an inducible *TRAF2* knock-down (KD) MM xenograft model. These data, coupled with RNA sequencing (RNA-seq) showing enrichment of ERK signaling in patients with MM at the time of relapse while on single-agent Len maintenance therapy, provide the framework for clinical trials of MEK inhibitors to overcome IMiD resistance and improve patient outcome in MM.

RESULTS

Genome-wide CRISPR-Cas9 screening identifies TRAF2 mediating IMiD sensitivity

We first carried out genome-wide CRISPR-Cas9 KO screening to identify genes and/or pathways mediating IMiD sensitivity (Fig. 1A and fig. S1, A and B). As expected, most of the positively selected genes are associated with activity of CRL4^{CRBN} E3 ligase, the main target of IMiDs mediating their anti-MM activity. Among these genes, we have previously validated that COP9 signalosome complex regulates sensitivity to IMiDs by modulating CRBN expression (31). TRAF2 was identified in our top 10 genes list (Fig. 1A and fig. S1A), and we demonstrated that three different single-guide RNAs (sgRNAs) targeting TRAF2 were enriched after IMiD treatment (Fig. 1, B and C). To confirm that TRAF2 modulates IMiD sensitivity, we individually cloned the TRAF2 sgRNAs into the LentiCRISPRv2 vector (38) and reintroduced them into MM cells. As expected, *TRAF2*-KO MM cells acquired notable resistance to Pom and Len treatment (Fig. 1, D and E, and fig. S2, A to C). Conversely, IMiD-resistant RPMI 8226 MM cell line showed increased sensitivity to Pom when TRAF2 was overexpressed (fig. S2D). In patient samples, TRAF2 mRNA was expressed in samples from patients relapsing on Len [Dana-Farber Cancer Institute (DFCI)/Intergroupe Francophone du Myelome (IFM)] and on other therapies (CoMMpass database) (fig. S2E).

However, TRAF2 immunohistochemical analysis of BM biopsies from six patients at the time of diagnosis with disease sensitive to Len compared to the time of relapse with disease resistant to single-agent Len maintenance demonstrated lower expression of TRAF2 protein in five of six samples at the time of relapse (Fig. 1F), suggesting that posttranslational modification of TRAF2 may account for clinical resistance. These data demonstrate that TRAF2 expression modulates sensitivity of MM cells to IMiDs.

Because previous studies showed that CRBN-IKZF1/3 axis plays a crucial role in IMiD-induced MM cell growth inhibition, we next examined whether *TRAF2* KO-induced IMiD resistance was CRL4^{CRBN} ligase activity dependent. *TRAF2* KO showed no effect on CRBN expression or IMiD-induced degradation of IKZF1/IKZF3 and down-regulation of interferon regulatory factor 4 (IRF4), the main effector of MM cell survival (Fig. 1G). Together, these data suggest that *TRAF2* KO-mediated IMiD resistance is independent of CRBN-IKZF1/3 axis.

TRAF2 KO induces activation of noncanonical NF- κ B and ERK pathways

We next investigated the molecular mechanism underlying IMiD resistance in *TRAF2* KO cells. *TRAF2* KO inhibited cleavage of caspase-3 and poly(ADP-ribose) polymerase (PARP) triggered by Pom and Len (Fig. 2, A and B, and fig. S3, A and B), indicating that *TRAF2* KO inhibits apoptotic cell death triggered by IMiDs. We further confirmed that TRAF2 was required for IMiD-induced cytotoxicity using CellTiter-Glo Luminescent Cell Viability Assay (Fig. 2C and fig. S3C) and flow cytometric analysis with annexin V staining (fig. S3D). Notably, *TRAF2* KO has no effect on MM cell growth and cell cycle (fig. S3, E and F). We also examined cross-resistance of *TRAF2* KO cells to other therapeutic agents. Viability assays showed that *TRAF2* KO cells were also resistant to dexamethasone and melphalan treatment (fig. S3G) but remained sensitive to bortezomib (BTZ) (fig. S3H). These data indicate that *TRAF2* KO-induced drug resistance is not specific to IMiDs and independent of ubiquitin-proteasome pathway.

We next performed RNA-seq to delineate signaling cascades mediating IMiD resistance induced by *TRAF2* KO. Both noncanonical NF- κ B (Fig. 2D, left) and ERK (Fig. 2D, right) pathways were enriched in *TRAF2* KO cells, consistent with previous reports that TRAF2 regulates NF- κ B and ERK signaling pathways (39). *TRAF2* KO cells showed significantly increased processing of precursor p100 to p52 (NF κ B2) (Fig. 2E and fig. S4A) and up-regulation of NF- κ B-inducing kinase (NIK) (fig. S4B), as well as activation of noncanonical NF- κ B pathway (fig. S4C), with minimal impact on p105 or p50 (NF κ B1) protein expression (fig. S4D). These results suggest that *TRAF2* KO predominantly activated noncanonical NF- κ B pathway. Consistent with RNA-seq analysis, we also confirmed that phosphorylation of ERK and upstream MEK were significantly up-regulated in *TRAF2* KO MM cells (Fig. 2F and fig. S4, E to G).

Noncanonical NF- κ B pathway mediates ERK pathway activation in TRAF2 KO cells

Because both noncanonical NF- κ B and MEK-ERK pathways were activated in *TRAF2* KO cells, we next examined interaction of these signaling pathways mediating IMiD resistance. p52 (NF κ B2) KO significantly reduced phosphorylation of MEK and ERK in *TRAF2* KO cells (Fig. 3A), suggesting that noncanonical NF- κ B pathway may regulate MEK-ERK activity in *TRAF2* KO cells. Moreover, p52

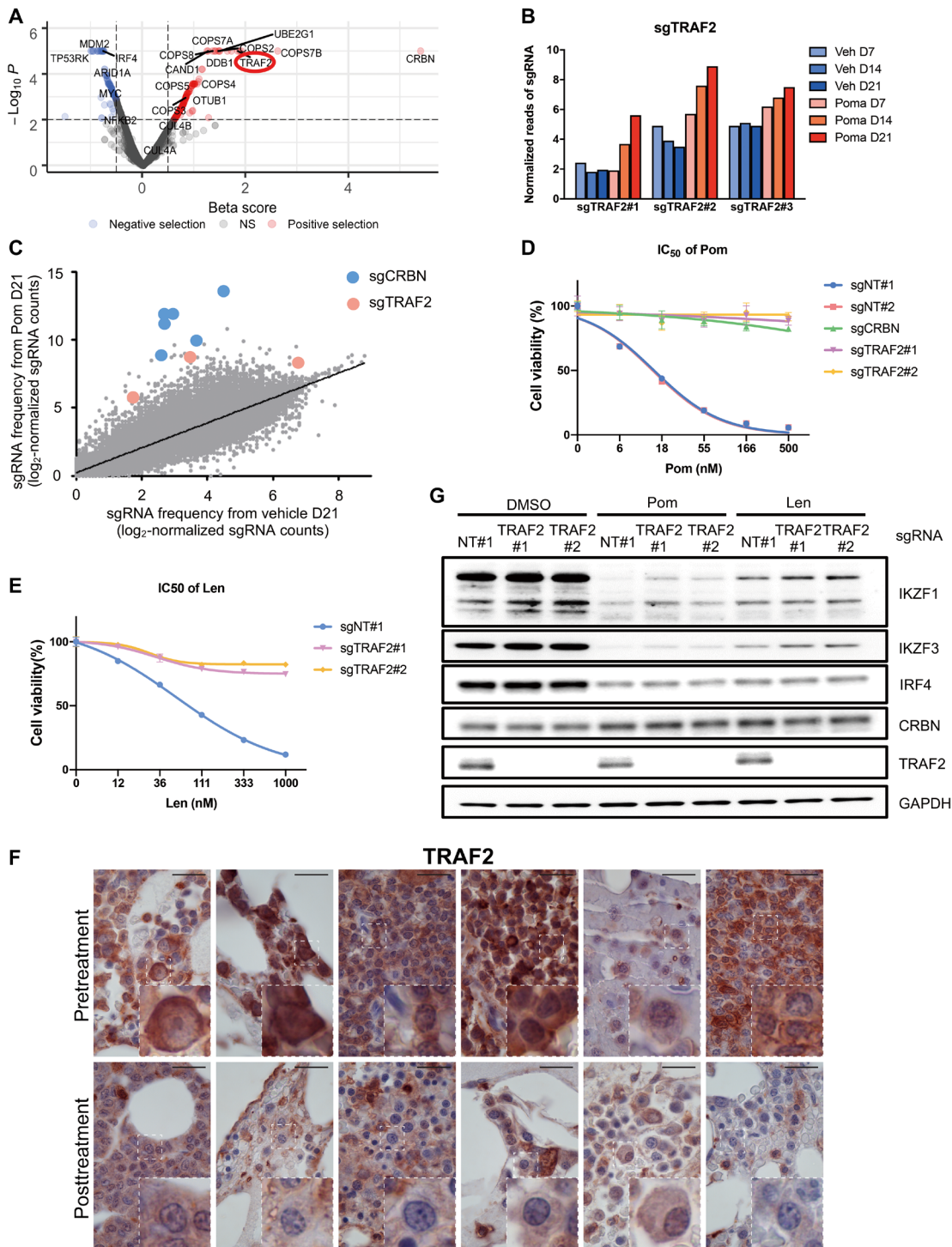


Fig. 1. Genome-wide CRISPR-Cas9 screen identifies TRAF2 to be required for antimyeloma activity of Pom. (A) Volcano plot showing both positively and negatively selected genes in the CRISPR-Cas9 screen at day 21 after Pom treatment. Genes shown in red and blue represent positively and negatively selected genes, respectively. NS, not significant. (B) Normalized reads of sgTRAF2 from cells treated with either dimethyl sulfoxide (DMSO) control or Pom at the indicated time points. Veh, DMSO control. (C) Enrichment of TRAF2 and CRBN sgRNAs after Pom treatment. Each dot specifies one sgRNA. (D and E) Dose-dependent survival of Pom-treated (D) and Len-treated (E) MM.1S cells infected with individually cloned lentiCRISPR viruses targeting the selected gene candidates. Controls were null-targeting lentiCRISPR viruses. Error bars represent SEM ($n = 3$). IC_{50} , half maximal inhibitory concentration. (F) Representative images of TRAF2 protein expression assessed by immunohistochemical staining of BM biopsies from six patients at time of diagnosis with disease sensitive to Len and at time of relapse with disease resistant to single-agent Len maintenance therapy. Scale bar, 20 μ m. (G) Representative Western blot analysis of control and TRAF2 KO MM.1S cells treated with DMSO, 0.5 μ M Pom, or 1 μ M Len for 72 hours. Whole-cell lysates (WCLs) were collected and probed with indicated Abs. GAPDH, glyceraldehyde-3-phosphate dehydrogenase; NT, non-targeting.

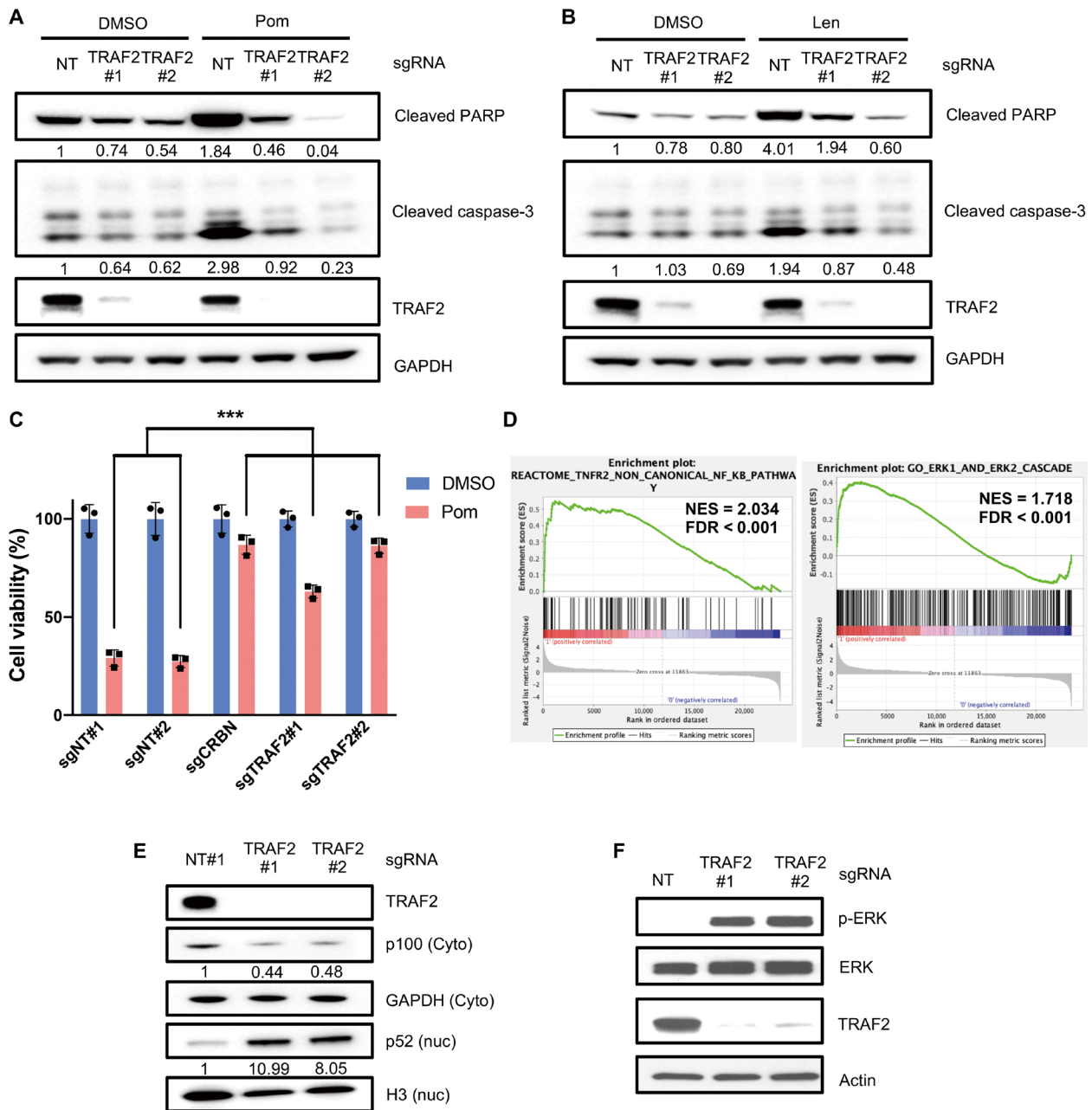


Fig. 2. TRAF2 KO inhibits apoptosis induced by IMiDs through enhancing noncanonical NF-κB and ERK pathway. (A and B) Representative Western blot analyses of control and TRAF2 KO MM.1S cells treated with DMSO or 1 μM Pom (A) or 1 μM Len (B) for 72 hours. WCLs were collected and probed with indicated Abs. (C) Percentage cell viability of control and TRAF2 KO MM.1S cells treated with 0.5 μM Pom for 72 hours. Cell viability was determined using CellTiter-Glo (CTG) cell viability assay. CRBN KO cells were analyzed as a positive control. Data are shown as means ± SEM. ***P < 0.001 by two-sided Student's *t* test. (D) Gene set enrichment analysis plots of datasets identified comparing TRAF2 KO and wild-type signatures. NES, normalized enrichment score. FDR, false discovery rate. (E) Nuclear and cytoplasmic protein were extracted from MM.1S TRAF2 KO cells and immunoblotted with indicated Abs. Cyto, cytoplasmic; nuc, nuclear. (F) WCLs from control and TRAF2 KO MM.1S cells were probed for p-ERK, ERK, and TRAF2 by immunoblotting. The numbers under the bands of blots indicate band intensity normalized to control.

KO in TRAF2 KO cells resensitized them to IMiD treatment (Fig. 3, B and C, and fig. S4H). To further confirm the role of up-regulation of phosphorylated MEK-ERK in resistance to IMiDs, we overexpressed p-ERK2 in IMiD-sensitive MM.1S cells, which conferred resistance to IMiDs (Fig. 3D and fig. S4I). Together, these results indicate that TRAF2 KO activates noncanonical NF-κB and

downstream MEK-ERK signaling mediating IMiD resistance in MM cells.

We next evaluated the clinical significance of ERK activation in relapsed MM patient samples. RNA-seq data from 69 MM patient samples demonstrated activated ERK pathway in 97% cases at the time of first relapse while receiving Len maintenance therapy

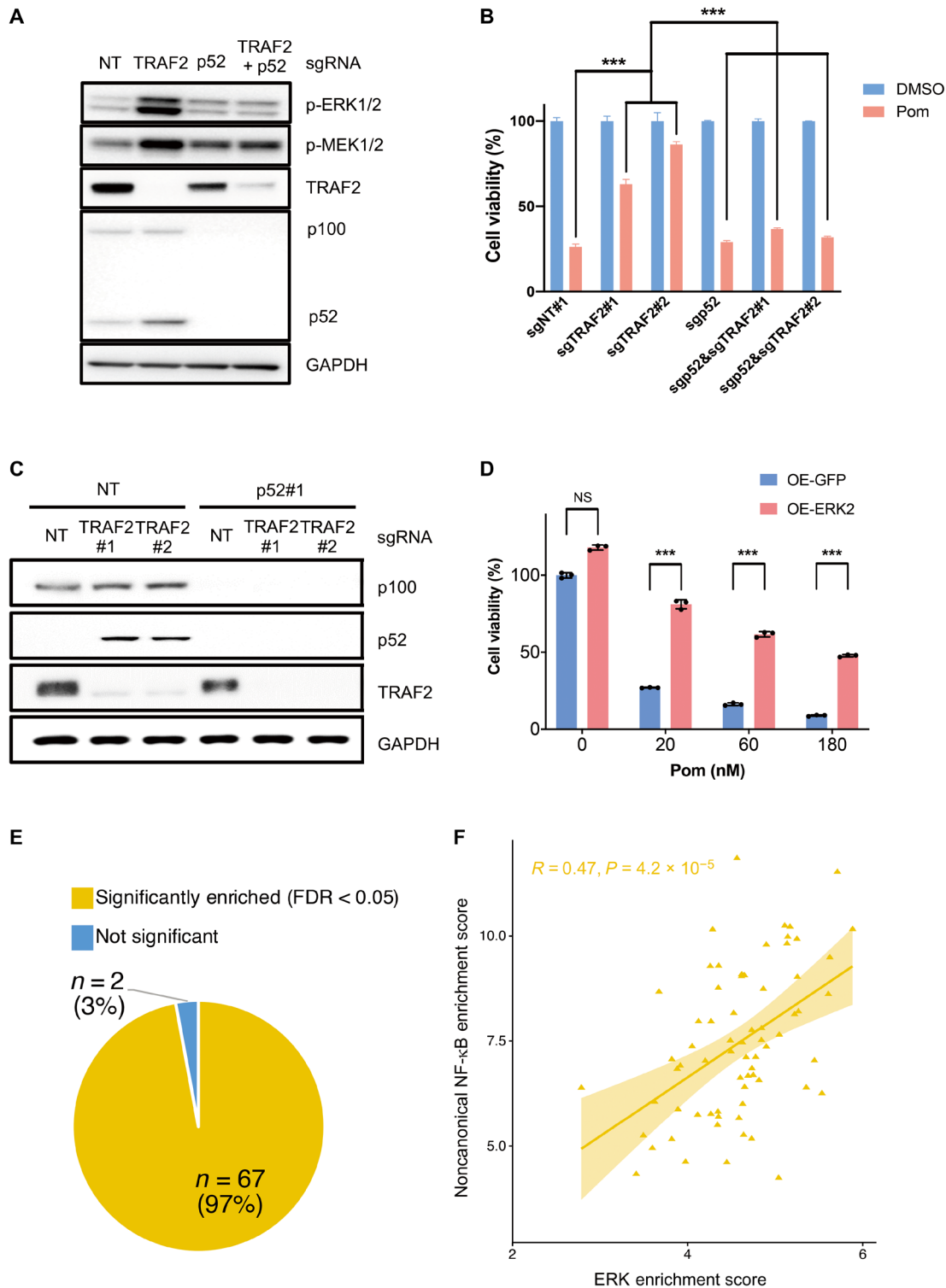


Fig. 3. Noncanonical NF-κB pathway mediates ERK pathway activation in TRAF2 KO cells. (A) Representative Western blot analysis of control and KO MM.1S cells. WCLs were collected and probed with indicated Abs. (B) Percentage cell viability of sgTRAF2 and/or sgp52 MM.1S cells treated with 0.5 μM Pom for 72 hours. Cell viability was determined using CTG assay. (C) KO efficiency of p100, p52, and TRAF2 in MM.1S cells was assessed by immunoblot analysis. (D) MM.1S cells were infected with lentivirus to constitutively express activated ERK2 and then treated with Pom (0 to 180 nM) for 72 hours. Cell viability was determined using CTG assay. Data in (B) and (D) are shown as means ± SEM. *** $P < 0.001$ by two-sided Student's t test. OE, over-expressed; GFP, green fluorescent protein. (E and F) RNA-seq data from MM patient samples of 69 patients at first relapse on Len maintenance therapy. Enrichment scores for ERK pathway activation (E) and correlation between ERK and noncanonical NF-κB pathway activation (F) were analyzed.

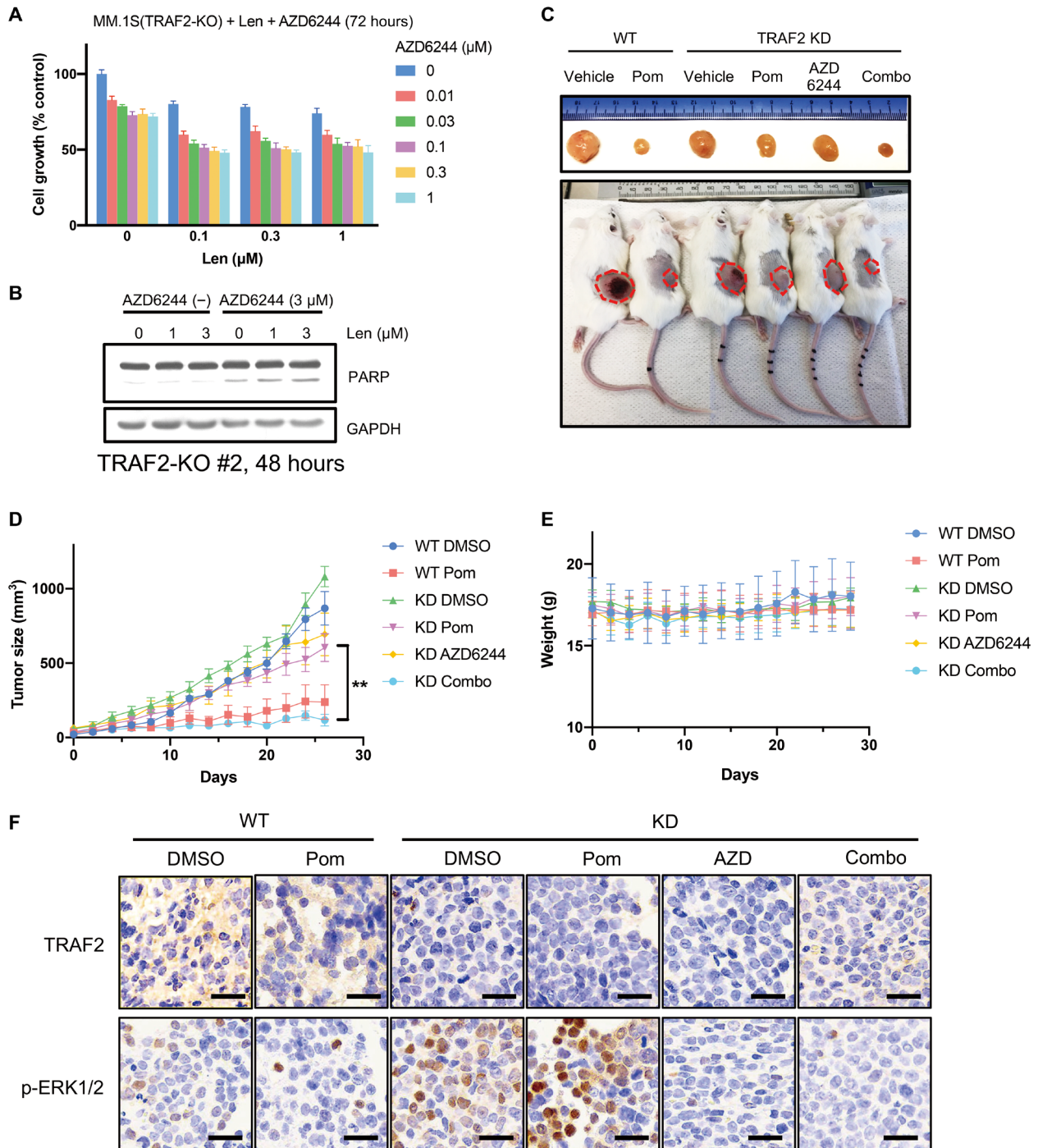


Fig. 4. Combination of AZD6244 with IMiDs triggers synergistic antimyeloma activity. (A) Percentage cell growth of *TRAF2* KO MM.1S cells after 3 days of treatment with Len (0 to 1 μM) and ERK inhibitor AZD6244 (0 to 1 μM). Cell growth was determined using 3-(4,5-dimethyl-2-thiazolyl)-2,5-diphenyl-2H-tetrazolium bromide (MTT) assay. (B) Representative Western blot analysis of *TRAF2* KO MM.1S cells treated for 48 hours with AZD6244 (0 to 3 μM), Len (0 to 3 μM), or both. WCLs were collected and probed with PARP Ab. (C to F) MM.1S cells expressing doxycycline-induced sh*TRAF2* were injected subcutaneously into CB-17 SCID mice ($n = 5$ for each group). When tumors reached 100 mm^3 , mice were randomized and treated with vehicle, Pom (2.5 mg/kg), AZD6244 (12.5 mg/kg), or both drugs for 3 weeks. (C) Macroscopic photographs after 21 days of therapy. (Photo credit: Jiye Liu, DFCI). Tumor volume (D) and body weight (E) were monitored over the indicated time period. Data in (D) and (E) are shown as means \pm SEM. $**P < 0.01$ by two-sided Student's *t* test. (F) Representative images of TRAF2 and p-ERK1/2 immunohistochemistry stain in tumor tissue sections from each group. Scale bars, 40 μm .

(Fig. 3E). There was also a significant positive correlation between ERK and noncanonical NF- κ B signaling in relapsed MM patient samples (Fig. 3F and fig. S4J). These data suggest a pivotal role of ERK activity in mediating IMiD resistance in the clinical setting.

Inhibition of MEK-ERK overcomes IMiD resistance induced by TRAF2 KD in vivo

Because we confirmed that ERK activity mediates IMiD resistance, we next sought to determine whether blockade of ERK pathway can overcome IMiD resistance induced by *TRAF2* KO. AZD6244 is a potent and highly selective MEK inhibitor (40), and we examined whether AZD6244 abrogated IMiD resistance in *TRAF2* KO cells. We first showed that AZD6244 in combination with IMiDs triggered synergistic cytotoxicity in MM.1S wild-type (WT) cells, evidenced by inhibition of cell proliferation (fig. S5, A and B). Addition of AZD6244 overcame resistance and mediated synergistic cytotoxicity with IMiDs in *TRAF2* KO MM cells, evidenced by decreased proliferation and p-ERK1/2, as well as by increased induction of PARP cleavage (Fig. 4, A and B, and fig. S5, C to E). To assess the efficacy of combination treatment in vivo, we first generated inducible *TRAF2* KD MM.1S cells and confirmed that *TRAF2* KD triggered activation of noncanonical NF- κ B and ERK pathways (fig. S5F)

and Pom resistance (fig. S5G) in vitro. These cells were then subcutaneously injected into severe combined immunodeficient (SCID) mice, allowing for induction of *TRAF2* KD by intraperitoneal injection of doxycycline. MM.1S WT cells were sensitive to Pom treatment, whereas MM.1S *TRAF2* KD cells demonstrated resistance. The combination of AZD6244 and Pom significantly reduced in vivo tumor growth of *TRAF2* KD cells, without associated host weight loss (Fig. 4, C to F). These data indicate that MEK inhibitor can abrogate activation of ERK1/2 and overcome IMiD resistance in vivo. Together, our results show that activation ERK signaling plays a crucial role modulating IMiD sensitivity and that MEK inhibitor can overcome ERK-mediated resistance and restore IMiD-induced MM cytotoxicity.

BM microenvironment induces IMiD resistance associated with down-regulation of TRAF2 and ERK activation

We and others have shown that the BM microenvironment plays an important role in promoting proliferation, survival, and drug resistance in MM cells (41). Specifically, we showed that either BMSCs or SC-sup activate NF- κ B and MEK-ERK pathways (37). We therefore next examined the relevance of *TRAF2* KO-induced ERK activation-mediated IMiD resistance in the context of the BM

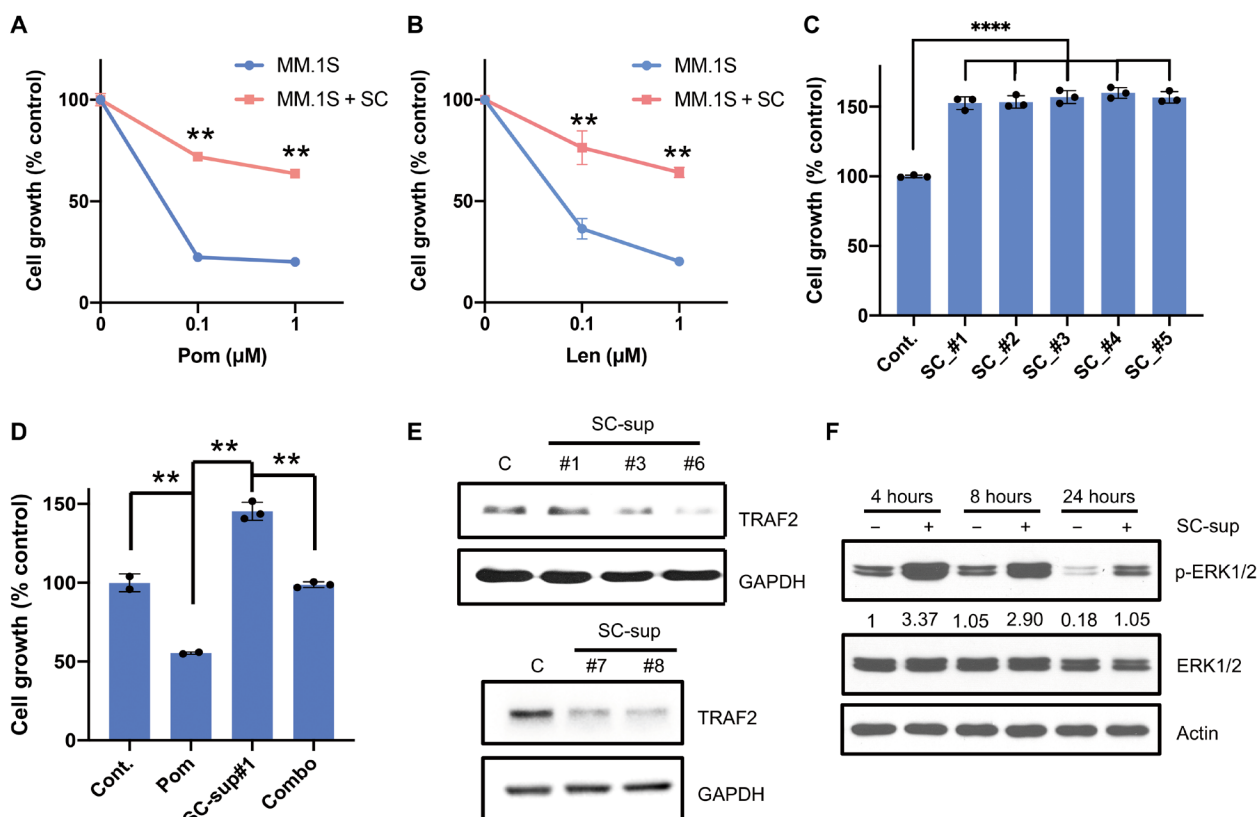


Fig. 5. BM microenvironment induces IMiD resistance through ERK pathway activation. (A and B) MM.1S cells were treated with indicated concentrations of Pom (A) or Len (B) in the presence or absence of BMSC. Cell growth was determined using MTT assay. (C) Percentage cell growth of MM.1S cells after 3 days culture with stromal cell supernatants (SC-sup). Cell growth (means \pm SEM) was determined using MTT assay and normalized to medium control. SCs were from five patients with MM. (D) Percentage cell growth of MM.1S cells after 3 days of treatment with Pom (1 μ M), SC-sup, or both. Cell growth was determined using MTT assay and normalized to the DMSO control group. (E) Immunoblot analysis of TRAF2 protein level in MM.1S cells cultured with SC-sup for 48 hours. SCs were from five patients with MM. (F) MM.1S cells were cultured for 0 to 24 hours in the presence or absence of SC-sup. WCLs were collected and probed with p-ERK1/2 and ERK1/2 Abs. The numbers under the bands of blots indicate band intensity normalized to control. Data in (A) to (D) are shown as means \pm SEM. **** P < 0.0001 and ** P < 0.01 by two-sided Student's *t* test.

microenvironment. As expected, coculture of MM cells with BMSCs (Fig. 5, A and B, and fig. S6, A and B) conferred resistance to IMiDs. Moreover, BMSC supernatants (SC-sup) similarly enhanced MM cell growth and conferred resistance to IMiDs (Fig. 5, C and D, and fig. S6C) associated with down-regulation of TRAF2 (Fig. 5E) and up-regulation of p-ERK (Fig. 5F). These data suggest that IMiD resistance in the BM microenvironment can be mediated, at least in part, by TRAF2 down-regulation-induced ERK activation.

ERK activation mediates IMiD resistance

To further delineate the mechanism whereby SC-sup confers IMiD resistance, we next performed cytokine array analysis and identified that TNF- α and IL-6 were highly secreted by BMSCs (Fig. 6A). TNF- α , but not IL-6, treatment induced TRAF2 down-regulation in MM cell lines (Fig. 6, B and C) and patient MM cells (Fig. 6D). TNF- α significantly inhibited IMiD-induced MM cytotoxicity in a dose-dependent manner (Fig. 6E and fig. S7, A to C), and similar to

TRAF2 KO, TNF- α induced IMiD resistance by activating ERK and noncanonical NF- κ B pathways (fig. S7, D and E), without altering CRBN expression (fig. S7F).

To further define the mechanism of TNF- α -mediated TRAF2 down-regulation, we next showed that TNF- α promoted TRAF2 protein degradation in a time- and dose-dependent manner (Fig. 6F and fig. S8A) and that the half-life of TRAF2 was markedly shortened by TNF- α treatment (fig. S8B). Because previous studies identified TRAF2 as a substrate of the proteasome (42), we also treated MM cells with TNF- α in the presence or absence of proteasome inhibitor BTZ or carfilzomib (CFZ). Notably, TRAF2 down-regulation triggered by TNF- α was inhibited by these proteasome inhibitors (Fig. 6G), associated with accumulation of ubiquitinated TRAF2 (Fig. 6H). These data confirm that TNF- α -induced TRAF2 down-regulation is due, at least in part, to its proteasomal degradation in MM cells. As described above, TRAF2 KO induced MEK-ERK phosphorylation via noncanonical NF- κ B activation, resulting in IMiD resistance. Consistent with a previous study (43), we also show that TNF- α also triggered

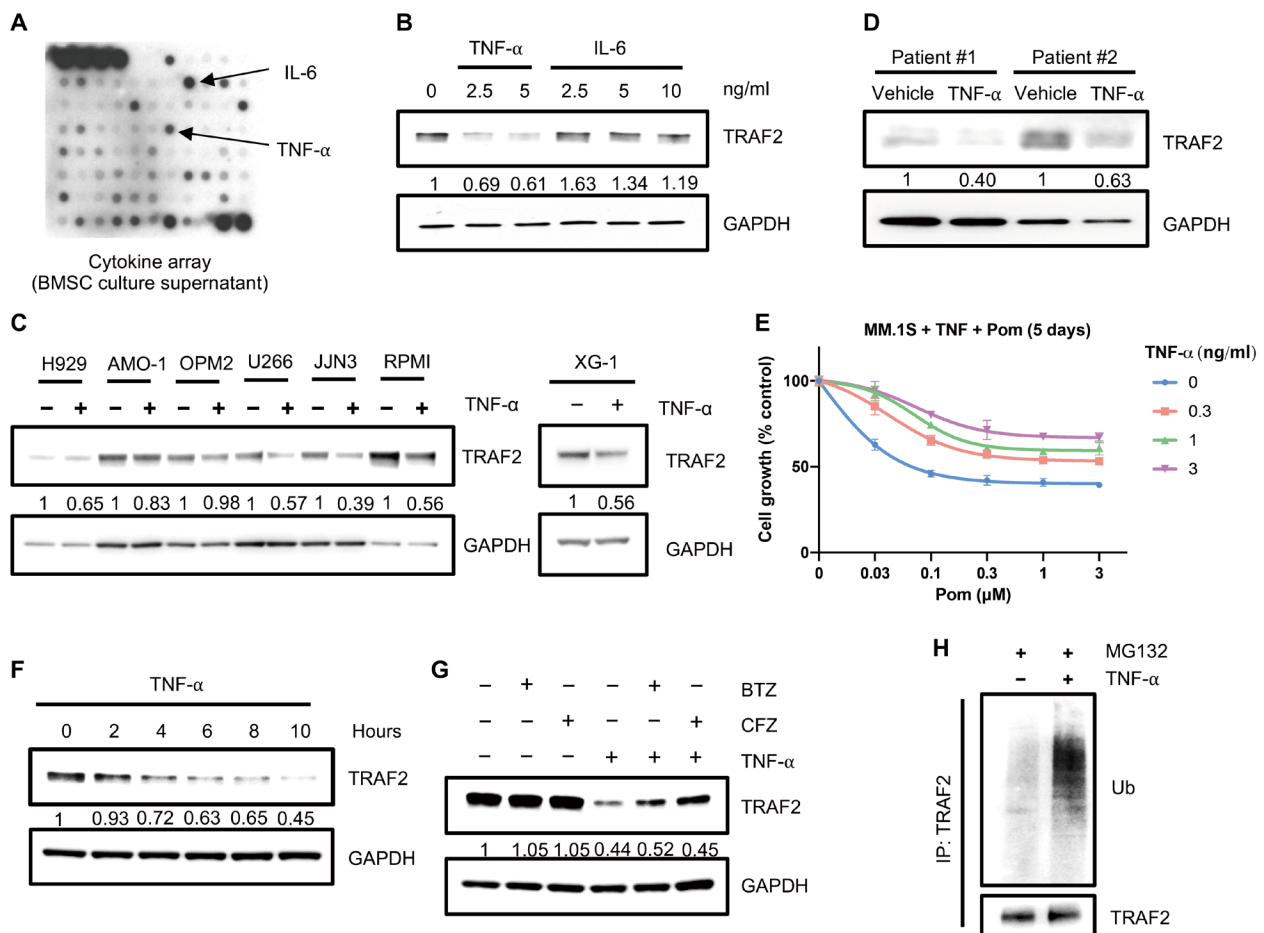


Fig. 6. Paracrine TNF- α in stromal cell supernatant induces IMiD resistance through proteasomal degradation of TRAF2. (A) Representative image of cytokine Ab array screening of SC-sup. Supernatant was collected after 24-hour culture with BMSCs and filtered by a 0.22 μ m low-protein binding membrane. (B) Representative Western blot analysis of MM.1S cells treated with TNF- α or IL-6 for 24 hours. WCLs were collected and probed with TRAF2 Ab. (C) MM cell lines were treated with TNF- α (5 ng/ml) for 48 hours. Cell lysates were collected and blotted with TRAF2 Ab. (D) Immunoblot analysis of patient MM cells treated with TNF- α (5 ng/ml) for 48 hours. WCL was collected and probed with TRAF2 Ab. (E) Percentage cell growth of MM.1S cells after 5 days of treatment with Pom (0 to 3 μ M) and/or TNF- α (0 to 3 ng/ml). Cell growth (means \pm SEM) was determined using MTT assay. (F) MM.1S cells were treated with TNF- α (5 ng/ml) for 0 to 10 hours. WCLs were collected and probed with TRAF2 Ab. (G) MM.1S cells were treated with 0.5 nM BTZ or 2.5 nM CFZ for 2 hours, followed by treatment with TNF- α (10 ng/ml) for 24 hours. WCLs were collected and probed with TRAF2 Ab. (H) MM.1S cells were cultured with TNF- α (5 ng/ml) for 18 hours and then treated with MG132 (10 μ M) for 6 hours. WCLs were collected and immunoprecipitated by anti-TRAF2 Ab and probed for polyubiquitinated protein and TRAF2. IP, immunoprecipitated. The numbers under the bands of blots indicate band intensity normalized to control.

ERK phosphorylation (fig. S7D). Last, we and others have shown that IL-6 activates ERK signaling and resistance to dexamethasone-induced MM cell apoptosis (44). Here, we show that IL-6 also directly induces IMiD resistance (Fig. 7A). In contrast, IGF-1 α does not trigger ERK activation or IMiD resistance (fig. S9). These data therefore indicate that soluble factors which induce MEK-ERK activation can protect MM cells from IMiD-induced cytotoxicity in the BM microenvironment.

Inhibition of MEK overcomes IMiD resistance induced by BM microenvironment

Because SC-sup (Fig. 5F), TNF- α (fig. S7D), and IL-6 (Fig. 7A) induced ERK phosphorylation and IMiD resistance in MM cells, we next determined whether MEK inhibitor was able to inhibit ERK1/2 phosphorylation and overcome IMiD resistance in the context of the BM microenvironment. We first showed that SC-sup-induced phosphorylation of ERK was completely blocked by a MEK inhibitor,

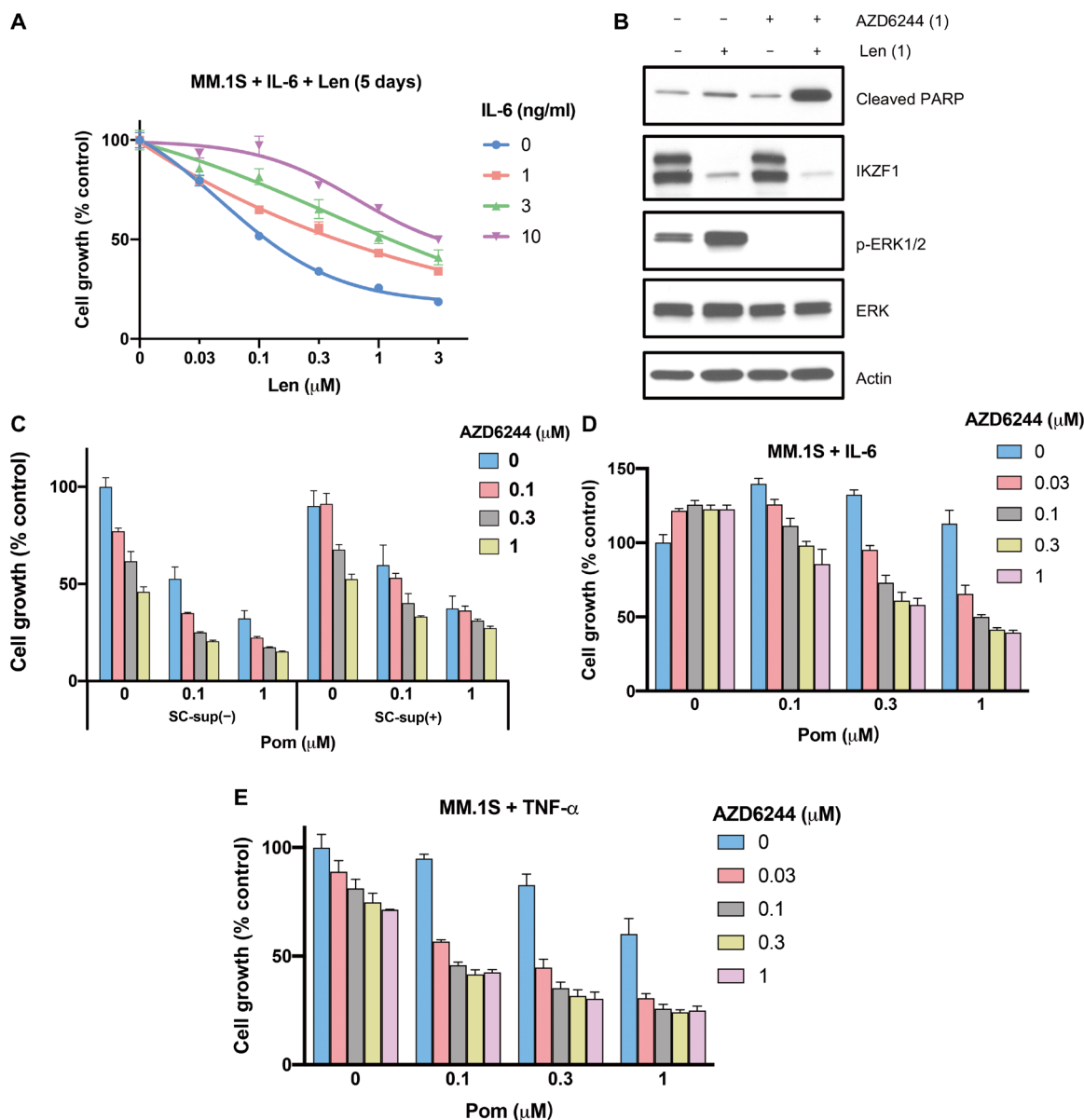


Fig. 7. AZD6244 overcomes IMiD resistance induced by BM microenvironment. (A) Percentage cell growth of MM.1S cells after 5 days of treatment with Len (0 to 3 μ M) and/or IL-6 (0 to 10 ng/ml). Cell growth (means \pm SEM) was determined using MTT assay. (B) Representative Western blot analysis of MM.1S cells cultured for 72 hours in the presence of BMCS with AZD6244 (1 μ M), Len (1 μ M), or both. WCLs were collected and probed with anti-cleaved PARP, IKZF1, p-ERK, and ERK Abs. (C) Percentage MM.1S cell growth in cultures with or without SC-sup after 5 days of treatment with Pom (0 to 1 μ M), AZD6244 (0 to 1 μ M), or both. Cell growth (means \pm SEM) was determined using MTT assay. (D) Percentage MM.1S cell growth in cultures with IL-6 (5 ng/ml) after 5 days of treatment with Pom (0 to 1 μ M), AZD6244 (0 to 1 μ M), or both. Cell growth (means \pm SEM) was determined using CTG assay. (E) Percentage MM.1S cell growth in cultures with TNF- α (5 ng/ml) after 5 days of treatment with Pom (0 to 1 μ M), AZD6244 (0 to 1 μ M), or both. Cell growth (means \pm SEM) was determined using CTG assay.

AZD6244 (Fig. 7B). Moreover, PARP cleavage was markedly enhanced by combination treatment of Pom with AZD6244, without affecting IKZF1 degradation (Fig. 7B). Addition of AZD6244 overcame resistance to Pom and Len in SC-sup-treated MM cells (Fig. 7C and fig. S10, A and B). We also observed that IMiD resistance triggered by IL-6 or TNF- α was similarly abrogated by AZD6244 (Fig. 7, D and E). These data indicate that MEK-ERK inhibitor can overcome IMiD resistance triggered by TNF- α and IL-6 in SC-sup and restore MM cell sensitivity to IMiD treatment in the BM milieu.

DISCUSSION

During the past two decades, IMiDs have demonstrated remarkable anti-MM activity when used alone or combined with proteasome inhibitors and/or monoclonal Abs as initial, salvage, and maintenance therapies (7, 25, 26, 45, 46). More potent IMiDs with enhanced affinity to CRBN have recently been developed to even further increase their clinical efficacy (47–49). Moreover, we and others (24) have also identified novel binding protein of IMiDs, such as TP53-regulating kinase, which may broaden their clinical utility. However, most MM cells eventually acquire resistance to IMiDs, which has, to date, been attributed to decreased expression of CRBN and rarely CRBN mutations (50, 51). Defining mechanisms underlying clinical resistance to IMiDs is therefore essential to inform the design of novel strategies to restore and/or enhance IMiD sensitivity and improve patient outcome.

Targeted genome editing technologies have transformed our abilities to discover basic biological mechanisms underlying specific phenotypes (52, 53). Specifically, the development of the CRISPR-Cas9 system and Cas9-based functional genetic screening tools has facilitated the identification of genes essential for drug resistance (54, 55), and we have used genome-wide CRISPR-Cas9 KO screening to delineate mechanisms of IMiD resistance in MM. We found that many CRL4^{CRBN} E3 ubiquitin ligase-associated genes are enriched in positively selected genes, confirming that CRBN pathway genes mediate sensitivity of MM to IMiDs. Conversely, many genes essential for MM survival and proliferation (31, 56–58) are depleted in negatively selected genes. From this screening, we previously identified the signalosome (CSN) family genes to be positively enriched, and validated that CSN genes regulate CRBN expression, suggesting that strategies to up-regulate CSN may restore CRBN levels and IMiD sensitivity (31). In the current study, we identified TRAF2 as one of the top 10 genes positively selected in our genome-wide CRISPR-Cas9 KO screening. TRAF2 is a member of the TRAF protein family functions as a component of TNF receptor complex and mediates activation of NF- κ B and/or ERK pathways (59, 60). It also functions as a RING domain E3 ligase that is activated by sphingosine-1-phosphate and catalyzes the lysine-63-linked poly-ubiquitination of receptor interacting serine/threonine kinase 1 (RIP1), thereby leading to NF- κ B activation (61).

An integrated analysis from 155 MM samples identified that inactive mutations of TRAF2 result in constitutive activation of noncanonical NF- κ B pathway (62). Here, we show that TRAF2 KO significantly induces IMiD resistance, thereby identifying TRAF2 as an essential mediator of IMiD sensitivity in MM cells. However, TRAF2 KO does not alter CRBN expression or IMiD-induced degradation of IKZF1/3 and its downstream targets IRF4 and c-Myc. Our data therefore identify a novel mechanism underlying IMiD resistance, independent of the CRBN-IKZF1/3 axis. We show that

IMiD resistance in TRAF2 KO cells is mediated by noncanonical NF- κ B and its downstream ERK signaling and that MEK inhibitor AZD6244 can restore sensitivity to IMiDs in vitro and in vivo using our inducible TRAF2 KD MM model. This is of great potential clinical interest, because our analyses of RNA-seq data show nearly universal activation of ERK signaling in MM patient samples at the time of first relapse while on Len maintenance therapy, suggesting that ERK inhibitor may restore IMiD sensitivity in the clinic.

We and others have shown that BMSCs and accessory cells (plasmacytoid dendritic cells, myeloid-derived suppressor cells, osteoclasts, and T regulatory cells) in the MM BM microenvironment play a crucial role in MM pathogenesis by promoting tumor cell growth, survival, and immunosuppression, as well as conferring drug resistance. These biologic sequelae are due to direct tumor cell–BMSC/accessory cell interaction (35) and/or secretion of soluble factors including IL-6, TNF- α , IGF-1 α , and vascular endothelial growth factor (63, 64) in the BM milieu. Moreover, our early studies showed that TNF- α can directly stimulate the production of IL-6 and up-regulate adhesion molecules (65), thereby further promoting tumor/accessory cell interactions. Here, we show that SC-sup, IL-6, and TNF- α induce IMiD resistance in MM cells mediated via ERK signaling. Although IL-6 directly activates ERK signaling, we show that TNF- α triggers proteasomal degradation of TRAF2 and activation of noncanonical NF- κ B, with downstream ERK pathway activation. In contrast, IGF-1 neither activates ERK signaling nor triggers IMiD resistance. Therefore, ERK pathway signaling is implicated in mediating IMiD resistance triggered by multiple stimuli in the BM milieu. Combination MEK inhibitor AZD6244 with IMiDs overcomes resistance to Pom and Len conferred by the BM milieu.

In summary, we have identified and validated that activation of MEK-ERK pathway directly by soluble factors (i.e., IL-6) or indirectly by activation of TRAF2 degradation-induced noncanonical NF- κ B activation mediates IMiD resistance in the BM microenvironment. These studies not only delineate a novel CRBN-independent mechanism of IMiD resistance in the BM milieu but also provide the preclinical rationale for combining inhibitors of MEK/ERK signaling with Len or Pom to overcome IMiD resistance and improve patient outcome in MM.

MATERIALS AND METHODS

Cells and culture conditions

MM.1S, RPMI 8226, H929, U266, and human embryonic kidney (HEK) 293T cells were purchased from the American Type Culture Collection. AMO-1, JFN-3, OPM2, and KMS-12BM cells were purchased from Deutsche Sammlung von Mikroorganismen und Zellkulturen (DSMZ). All cell lines were verified by short tandem repeat (STR) DNA fingerprinting analysis (Molecular Diagnostic Laboratory, DFCI) and tested for mycoplasma using the MycoAlert Mycoplasma Detection Kit (Lonza). All cells were grown at 37°C in 5% CO₂ condition: MM.1S, RPMI 8226, H929, U266, AMO-1, JFN-3, OPM2, and KMS-12BM cells were maintained in RPMI 1640 medium; HEK293T cells were maintained in Dulbecco's modified Eagle's medium. All media were supplemented with 10% fetal bovine serum (FBS), 1 \times antibiotic-antimycotic, 1 \times GlutaMAX, and 1 \times Heps.

Primary MM cells and BMSCs

BM samples were obtained from patients with MM after informed consent and approval by the Institutional Review Board of the DFCI.

Mononuclear cells were separated by Ficoll-Paque PLUS (GE Healthcare Life Sciences). MM cells were purified by CD138-positive selection with human CD138 MicroBeads (Miltenyi). Long-term BMSCs were established by culturing CD138-negative BM mononuclear cells for 4 to 6 weeks in RPMI 1640 medium supplemented with 10% FBS and 1× antibiotic-antimycotic.

Generation and collection of SC-sup

The culture medium of established BMSCs was replaced with fresh complete medium. Supernatant was collected 24 hours later, followed by centrifugation at 2000 rpm for 10 min to clear cells and debris. Filtration was then performed with a 0.22 μM low-protein binding membrane (Millipore Sigma).

Reagents and Abs

Len, Pom, BTZ, CFZ, and MG132 were purchased from Selleck Chemicals; AZD6244 was purchased from Cayman Chemical. All were dissolved in dimethyl sulfoxide (DMSO) and stored at −20°C for up to 6 months. For all cell-based experiments, drugs were diluted at least by 1:1000 to ensure that the final DMSO concentration was lower than 0.1%. Cycloheximide solution was purchased from Millipore Sigma. Human recombinant TNF-α and IL-6 were purchased from STEMCELL Technologies. Doxycycline was purchased from Boston Bioproducts. Abs were obtained as follows: IKZF1 (no. 5443, Cell Signaling Technology), IKZF3 (no. 15103, Cell Signaling Technology), IRF4 (no. 4299, Cell Signaling Technology), CRBN (no. SAB045910, Sigma-Aldrich), TRAF2 (no. 4724, Cell Signaling Technology and no. ab126758, Abcam), glyceraldehyde-3-phosphate dehydrogenase (no. 5174, Cell Signaling Technology), cleaved PARP (no. 5625, Cell Signaling Technology), caspase-3 (no. 14220, Cell Signaling Technology), NF-κB2 p100/p52 (no. 4882, Cell Signaling Technology), histone H3 (no. 4499, Cell Signaling Technology), phospho-NF-κB2 p100 (Ser866/870) (no. 4810, Cell Signaling Technology), ubiquitin (no. 3936, Cell Signaling Technology), p44/42 MAPK (Erk1/2) (no. 4695, Cell Signaling Technology), phospho-p44/42 MAPK (Erk1/2) (Thr²⁰²/Tyr²⁰⁴) (no. 4370, Cell Signaling Technology), pan-actin (no. 8456, Cell Signaling Technology), NF-κB1 p105/p50 (no. 3035, Cell Signaling Technology), lamin A/C (no. 4777, Cell Signaling Technology), anti-rabbit immunoglobulin G (IgG), horseradish peroxidase (HRP)-linked Ab (no. 7074, Cell Signaling Technology), and anti-mouse IgG, HRP-linked Ab (no. 7076, Cell Signaling Technology). Protein G Sepharose was purchased from Millipore Sigma.

RNA sequencing

For RNA-seq, total RNA of WT and *TRAF2* KO cells was extracted using the RNeasy Mini Kit (Qiagen). Library was prepared, and samples were sequenced on NovaSeq 6000 PE150. RNA-seq datasets were aligned to human reference genome hg38 using Homo sapiens steroidogenic acute regulatory protein (STAR). RNA-seq by expectation-maximization was used to do the transcript quantification, and differential expression analysis was performed with DESeq2. Gene set enrichment analysis (GSEA) was performed to identify significantly enriched pathways. The biologically defined gene sets were obtained from the Molecular Signatures Database (<http://software.broadinstitute.org/gsea/msigdb/index.jsp>). Genes used for GSEA analysis were preranked on the basis of log₂ fold change of TPM (transcripts per kilobase million) between WT and *TRAF2* KO cells.

CellTiter-Glo cell viability assay

Cells were plated in medium (8000 cells per well, 100-μl final volume) in white, 96-well opaque plates (no. 3917, Corning). Cells were incubated for indicated intervals at 37°C in a 5% CO₂ incubator. Assay plates were removed from the incubator and equilibrated to room temperature before addition of 50 μl of CellTiter-Glo reagent (Promega), according to the manufacturer's instructions. Plates were shaken on an orbital shaker for 2 min at 500 rpm and then incubated at room temperature on the bench top for at least 10 min. Luminescence was detected using a spectrophotometer (SpectraMax M3, Molecular Devices).

Cell growth assay

The growth-inhibitory effect was assessed by measuring 3-(4,5-dimethyl-2-thiazolyl)-2,5-diphenyl-2*H*-tetrazolium bromide (MTT) (Sigma-Aldrich) dye absorbance, as previously described (56). Cells were cultured in 96-well plates (100 μl) with or without drug treatment; for the last 4 hours, cells were pulsed with 10 μl of MTT, followed by addition of 100 μl of isopropanol containing 0.04 N HCl. Absorbance was measured at 570 nm, with 630 nm as a reference wavelength, using a spectrophotometer (SpectraMax M3, Molecular Devices).

Immunoblot analysis

Cells were treated, harvested, washed with phosphate-buffered saline, and lysed in radioimmunoprecipitation assay buffer (no. R0278, Millipore Sigma) containing protease inhibitor and phosphatase inhibitor (no. 78440, Thermo Fisher Scientific). The suspension was incubated for 15 min on ice and vortexed for 5 min. Then, samples were centrifuged at 13,000 rpm at 4°C for 10 min. The supernatant was used as whole-cell lysates. Protein concentrations were quantified with a BCA protein assay kit (no. 23227, Thermo Fisher Scientific). Samples were mixed with 4× LDS sample buffer (no. NP0007, Thermo Fisher Scientific), and boiled at 95°C for 8 min. Equal amounts of protein were run on NuPAGE Bis-Tris gels (Thermo Fisher Scientific) at a constant voltage. Proteins were transferred onto nitrocellulose membrane by iBlot Gel Transfer Device (Thermo Fisher Scientific). Then, the membranes were blocked in 5% nonfat dry milk for 1 hour at room temperature and incubated with primary Abs in 5% bovine serum albumin at 4°C overnight. Blots were then washed three times with 1× Tris Buffered Saline with Tween (TBS-T), before incubation with secondary Abs for 1 hour. SuperSignal chemiluminescent substrate (Thermo Fisher Scientific) was used for signal detection. For reblotting the membranes, blots were stripped in stripping buffer (no. 46428, Thermo Fisher Scientific) according to the manufacturer's instruction and reblocked. The intensity of band was quantified by ImageStudio (LI-COR).

Viral production

On day 0, HEK293T cells were plated in a T150 flask. On day 1, for each flask, 20 μg of lentiviral vector, 15 μg of psPAX2 (no. 12260, Addgene), and 10 μg of pMD2.G (no. 12259, Addgene) diluted in 3 ml of Opti-MEM were combined with 150 μl of Lipofectamine 2000 diluted in 3 ml of Opti-MEM. The mixture was left for 20 min and then added to the cells. Twelve hours after transfection, the medium was replaced by fresh complete medium. The supernatant containing virus was collected 72 hours after transfection, followed by centrifugation at 2000 rpm for 10 min to pellet cell debris. Filtration was then performed with a 0.45-μm low-protein binding membrane (no. SE1M003M00, Millipore). Then, the virus was concentrated by the Lenti-X Concentrator (no. 631231, Takara).

Generation of stable cell lines

For generation of CRISPR KO cell lines, oligonucleotides (table S1) targeting different genes were annealed and subcloned into LentiCRISPRv2 vectors (38). Constructs were packaged into lentivirus in HEK293T cells. Target cells were seeded in 12-well plates and spininfected with virus for 1.5 hours at 2000 rpm at 35°C, supplemented with Polybrene (8 µg/ml). Medium was then aspirated, and fresh complete medium was added to exclude Polybrene. After 1 day, cells were selected for stable KO using puromycin (0.5 µg/ml). After 7 days, cells were collected for immunoblotting or other experiments. To generate inducible TRAF2 KD cells for in vivo study, the SMARTvector inducible human TRAF2 lentivirus plasmid (Horizon Dharmacon) was transfected into HEK293T cells with packaging vectors. Cells were spininfected for 1 hour with viral particles at 2000 rpm at 35°C, supplemented with Polybrene (8 µg/ml). After 1 day, cells were selected with puromycin (0.5 µg/ml) for 7 days. For the constitutive expression of ERK2-MEK1 fusion protein, the sequence of full length of ERK2-MEK1 was cloned from pCMV-myc-ERK2-L4A-MEK1_fusion vector (no. 39197, Addgene) into plenti-CMV-Puro-DEST (no. 17452, Addgene). The expression plasmid was transfected into HEK293T cells with the packaging vectors. Cells were spininfected for 1.5 hours with viral particles at 2000 rpm at 35°C, supplemented with Polybrene (8 µg/ml). After 1 day, cells were selected with puromycin (0.5 µg/ml) for 7 days.

Human cytokine array

The cytokine array assay was performed using a Human Cytokine Array C5 kit (no. AAH-CYT-5-2, RayBiotech), according to the manufacturer's instruction.

In vivo ubiquitination assay

MM cells were treated with TNF-α (5 ng/ml) for 24 hours and then 10 µM MG132 for 6 hours. Cells were lysed in IP lysis buffer (no. 87787, Thermo Fisher Scientific). TRAF2 protein was pulled down by Protein G Agarose with TRAF2 Ab overnight at 4°C and washed with IP lysis buffer. Protein was eluted by incubation with LDS loading buffer at 100°C for 5 min, separated by SDS-polyacrylamide gel electrophoresis, transferred to nitrocellulose membrane, and probed with indicated Abs.

Cycloheximide chase assay

Cells were cultured in 12-well plates with or without TNF-α and treated with cycloheximide (100 µg/ml) for the indicated time periods before harvest. Cell lysates were analyzed by Western blotting.

Mouse xenograft assays

A total of 6×10^6 Tet-inducible *TRAF2* KD MM.1S cells were suspended in 100 µl of RPMI 1640 medium and injected into the flanks of 200 cGy-irradiated female SCID mice. Tumor size was measured every 2 days with an electrical caliper. The tumor volume was determined with the formula: $(\text{length} \times \text{width}^2) \times 0.5$, where length is the longest diameter and width is the shortest diameter. When the tumor volume reached 100 to 150 mm³, xenografted mice were randomized to treatment and control cohorts. In the *TRAF2* KD group, mice received doxycycline (2.5 mg/kg) via intraperitoneal injection to induce *TRAF2* KD. AZD6244 (12.5 mg/kg per day) and Pom (2.5 mg/kg for 5 days/week) administered by oral gavage. All care and treatment of experimental animals was conducted under a protocol

approved by DFCI Institutional Animal Care and Use Committee guidelines. All mice were housed in a pathogen-free environment at a DFCI animal facility and were handled in strict accordance with Good Animal Practice, as defined by the Office of Laboratory Animal Welfare.

Cell cycle assay

Cells were harvested and concentrations adjusted to 1×10^6 cells/ml. After washing, cells were suspended in 50 µl of Hanks' balanced salt solution (HBSS) containing 2% FBS; 1 ml of ice-cold 70% ethanol was then added in a dropwise manner while mixing gently on a vortex, with storage on ice for no less than 2 hours. Pelleted cells were washed with HBSS containing 2% FBS twice, and then 1 ml of 4',6-diamidino-2-phenylindole (DAPI) working solution was added, followed by incubation in the dark for 15 to 30 min at room temperature. Cells were filtered through a 40-µm mesh filter and then analyzed by flow cytometry.

Annexin V and LIVE/DEAD Aqua staining

MM cells (1×10^6) were treated with Pom for 5 days and then stained with the LIVE/DEAD Fixable Aqua Dead Cell Staining Kit (no. L34957, Thermo Fisher Scientific) and annexin V-phycoerythrin conjugate (no. 640908, BioLegend), according to the manufacturer's instruction. Cells were analyzed in BD FACSCanto II (BD Biosciences) using the FACSDiva software (BD Biosciences).

Immunohistochemistry

Tissue specimen sections of formalin-fixed, paraffin-embedded BM biopsies from six patients at diagnosis with MM sensitive to Len and at the time of relapse with disease resistant to single-agent Len were prepared and processed for immunohistochemistry to detect TRAF2 protein expression by using TRAF2 Ab (no. ab126758, Abcam). Tumor samples from mice were harvested and fixed in formalin and then embedded in paraffin and cut in 4 µm sections. Sections were stained with TRAF2, p-ERK1/2, and DAPI. Tissues were imaged using a microscope.

Analysis of RNA-seq data from patient samples

RNA-seq data from 69 patients with MM at the time of first relapse while on single-agent Len maintenance (DFCI/IFM) were collected after study participants provided written informed consent. After RNA extraction, RNA quantity was evaluated, and only samples with ≥ 100 ng of RNA with RNA integrity number (RIN) value ≥ 7 were sequenced with stranded 50-base pair paired-end sequencing. After quality control, raw samples were quantified using Salmon and Gencode transcripts. Single-sample GSEA (ssGSEA), an extension of GSEA, was used to calculate separate enrichment scores for ERK pathway. R and ggpubr were used for statistical test and visualization. Pearson correlation analysis and Fisher's exact test were used for association analysis and enrichment in relapse samples. The DFCI/IFM and CoMMpass patient sample RNA-seq databases were used to analyze correlation between noncanonical NF-κB and ERK pathway activation in relapsed patient samples. TPM-level gene expression data were used only for patients who had CD138⁺ BM samples profiled at the time of relapse. We downloaded the Biocarta ERK pathway and Gene Ontology NIK NF-κB signaling pathways from the Molecular Signatures Database website, and with ssGSEA, we quantified the enrichment score for each patient. Spearman correlation between the two pathways were evaluated using R and ggpubr.

Statistical analysis

Student's *t* test or analysis of variance followed by Dunnett's test was used to compare differences between the treated group and the relevant control group. A value of $P < 0.05$ was considered significant.

SUPPLEMENTARY MATERIALS

Supplementary material for this article is available at <http://advances.sciencemag.org/cgi/content/full/7/23/eabg2697/DC1>

[View/request a protocol for this paper from Bio-protocol.](#)

REFERENCES AND NOTES

1. A. Palumbo, K. Anderson, Multiple myeloma. *N. Engl. J. Med.* **364**, 1046–1060 (2011).
2. P. G. Richardson, P. Sonneveld, M. W. Schuster, D. Irwin, E. A. Stadtmauer, T. Facon, J.-L. Harousseau, D. Ben-Yehuda, S. Lonial, H. Goldschmidt, D. Reece, J. F. San-Miguel, J. Blade, M. Boccadoro, J. Cavenagh, W. S. Dalton, A. L. Boral, D. L. Esseltine, J. B. Porter, D. Schenkein, K. C. Anderson; Assessment of Proteasome Inhibition for Extending Remissions (APEX) Investigators, Bortezomib or high-dose dexamethasone for relapsed multiple myeloma. *N. Engl. J. Med.* **352**, 2487–2498 (2005).
3. J. P. Fermand, P. Ravaud, S. Chevret, M. Divine, V. Leblond, C. Belanger, M. Macro, E. Pertuiset, F. Dreyfus, X. Mariette, C. Boccacio, J. C. Brouet, High-dose therapy and autologous peripheral blood stem cell transplantation in multiple myeloma: Up-front or rescue treatment? Results of a multicenter sequential randomized clinical trial. *Blood* **92**, 3131–3136 (1998).
4. S. Gandolfi, J. P. Laubach, T. Hideshima, D. Chauhan, K. C. Anderson, P. G. Richardson, The proteasome and proteasome inhibitors in multiple myeloma. *Cancer Metastasis Rev.* **36**, 561–584 (2017).
5. J. P. Laubach, P. Moreau, J. F. San-Miguel, P. G. Richardson, Panobinostat for the treatment of multiple myeloma. *Clin. Cancer Res.* **21**, 4767–4773 (2015).
6. P. G. Richardson, V. T. Hungria, S. S. Yoon, M. Beksac, M. A. Dimopoulos, A. Elghandour, W. W. Jedrzejczak, A. Guenther, T. N. Nakorn, N. Siritanaratkul, R. L. Schlossman, J. Hou, P. Moreau, S. Lonial, J. H. Lee, H. Einsele, M. Sopala, B. R. Bengoudifa, C. Corrado, F. Binlich, J. F. San-Miguel, Panobinostat plus bortezomib and dexamethasone in previously treated multiple myeloma: Outcomes by prior treatment. *Blood* **127**, 713–721 (2016).
7. S. Singhal, J. Mehta, R. Desikan, D. Ayers, P. Roberson, P. Eddlemon, N. Munshi, E. Anaissie, C. Wilson, M. Dhodapkar, J. Zeddis, B. Barlogie, Antitumor activity of thalidomide in refractory multiple myeloma. *N. Engl. J. Med.* **341**, 1565–1571 (1999).
8. P. L. McCarthy, K. Owzar, C. C. Hofmeister, D. D. Hurd, H. Hassoun, P. G. Richardson, S. Giralt, E. A. Stadtmauer, D. J. Weisdorf, R. Vij, J. S. Moreb, N. S. Callander, K. Van Besien, T. Gentile, L. Isola, R. T. Maziarz, D. A. Gabriel, A. Bashey, H. Landau, T. Martin, M. H. Qazilbash, D. Levitan, B. McClune, R. Schlossman, V. Hars, J. Postiglione, C. Jiang, E. Bennett, S. Barry, L. Bressler, M. Kelly, M. Seiler, C. Rosenbaum, P. Hari, M. C. Pasquini, M. M. Horowitz, T. C. Shea, S. M. Devine, K. C. Anderson, C. Linker, Lenalidomide after stem-cell transplantation for multiple myeloma. *N. Engl. J. Med.* **366**, 1770–1781 (2012).
9. M. Q. Lacy, S. R. Hayman, M. A. Gertz, A. Dispenzieri, F. Buadi, S. Kumar, P. R. Greipp, J. A. Lust, S. J. Russell, D. Dingli, R. A. Kyle, R. Fonseca, P. L. Bergsagel, V. Roy, J. R. Mikhael, A. K. Stewart, K. Laumann, J. B. Allred, S. J. Mandrekar, S. V. Rajkumar, Pomalidomide (CC4047) plus low-dose dexamethasone as therapy for relapsed multiple myeloma. *J. Clin. Oncol.* **27**, 5008–5014 (2009).
10. H. M. Lokhorst, T. Plesner, J. P. Laubach, H. Nahi, P. Gimsing, M. Hansson, M. C. Minnema, U. Lassen, J. Krejci, A. Palumbo, N. W. van de Donk, T. Ahmadi, I. Khan, C. M. Uhlar, J. Wang, A. K. Sasser, N. Losic, S. Lisby, L. Basse, N. Brun, P. G. Richardson, Targeting CD38 with daratumumab monotherapy in multiple myeloma. *N. Engl. J. Med.* **373**, 1207–1219 (2015).
11. S. Lonial, M. Dimopoulos, A. Palumbo, D. White, S. Grosicki, I. Spicka, A. Walter-Croneck, P. Moreau, M. V. Mateos, H. Magen, A. Belch, D. Reece, M. Beksac, A. Spencer, H. Oakervee, R. Z. Orlowski, M. Taniwaki, C. Rollig, H. Einsele, K. L. Wu, A. Singhal, J. San-Miguel, M. Matsumoto, J. Katz, E. Bleickardt, V. Poulart, K. C. Anderson, P. Richardson; ELOQUENT-2 Investigators, Elotuzumab therapy for relapsed or refractory multiple myeloma. *N. Engl. J. Med.* **373**, 621–631 (2015).
12. M. Attal, P. G. Richardson, S. V. Rajkumar, J. San-Miguel, M. Beksac, I. Spicka, X. Leleu, F. Schjesvold, P. Moreau, M. A. Dimopoulos, J. S. Huang, J. Minarik, M. Cavo, H. M. Prince, S. Mace, K. P. Corzo, F. Campana, S. Le-Guennec, F. Dubin, K. C. Anderson; ICARIA-MM study group, Isatuximab plus pomalidomide and low-dose dexamethasone versus pomalidomide and low-dose dexamethasone in patients with relapsed and refractory multiple myeloma (ICARIA-MM): A randomised, multicentre, open-label, phase 3 study. *Lancet* **394**, 2096–2107 (2019).
13. J. Knobloch, U. Ruther, Shedding light on an old mystery: thalidomide suppresses survival pathways to induce limb defects. *Cell Cycle* **7**, 1121–1127 (2008).
14. R. J. D'Amato, M. S. Loughnan, E. Flynn, J. Folkman, Thalidomide is an inhibitor of angiogenesis. *Proc. Natl. Acad. Sci. U.S.A.* **91**, 4082–4085 (1994).
15. Y. X. Zhu, K. M. Kortuem, A. K. Stewart, Molecular mechanism of action of immunomodulatory drugs thalidomide, lenalidomide and pomalidomide in multiple myeloma. *Leuk. Lymphoma* **54**, 683–687 (2013).
16. T. Hideshima, D. Chauhan, Y. Shima, N. Raj, F. E. Davies, Y. T. Tai, S. P. Treon, B. Lin, R. L. Schlossman, P. Richardson, G. Muller, D. I. Stirling, K. C. Anderson, Thalidomide and its analogs overcome drug resistance of human multiple myeloma cells to conventional therapy. *Blood* **96**, 2943–2950 (2000).
17. N. Mitsiades, C. S. Mitsiades, V. Poulaki, D. Chauhan, P. G. Richardson, T. Hideshima, N. C. Munshi, S. P. Treon, K. C. Anderson, Apoptotic signaling induced by immunomodulatory thalidomide analogs in human multiple myeloma cells: Therapeutic implications. *Blood* **99**, 4525–4530 (2002).
18. R. LeBlanc, T. Hideshima, L. P. Catley, R. Shringarpure, R. Burger, N. Mitsiades, C. Mitsiades, P. Cheema, D. Chauhan, P. G. Richardson, K. C. Anderson, N. C. Munshi, Immunomodulatory drug costimulates T cells via the B7-CD28 pathway. *Blood* **103**, 1787–1790 (2004).
19. G. Gorgun, M. K. Samur, K. B. Cowens, S. Paula, G. Bianchi, J. E. Anderson, R. E. White, A. Singh, H. Ohguchi, R. Suzuki, S. Kikuchi, T. Harada, T. Hideshima, Y. T. Tai, J. P. Laubach, N. Raj, F. Magrangeas, S. Minvielle, H. Avet-Loiseau, N. C. Munshi, D. M. Dorfman, P. G. Richardson, K. C. Anderson, Lenalidomide enhances immune checkpoint blockade-induced immune response in multiple myeloma. *Clin. Cancer Res.* **21**, 4607–4618 (2015).
20. A. Lopez-Girona, D. Mendy, T. Ito, K. Miller, A. K. Gandhi, J. Kang, S. Karasawa, G. Carmel, P. Jackson, M. Abbasian, A. Mahmoudi, B. Cathers, E. Rychak, S. Gaidarova, R. Chen, P. H. Schafer, H. Handa, T. O. Daniel, J. F. Evans, R. Chopra, Cereblon is a direct protein target for immunomodulatory and antiproliferative activities of lenalidomide and pomalidomide. *Leukemia* **26**, 2326–2335 (2012).
21. T. Ito, H. Ando, T. Suzuki, T. Ogura, K. Hotta, Y. Imamura, Y. Yamaguchi, H. Handa, Identification of a primary target of thalidomide teratogenicity. *Science* **327**, 1345–1350 (2010).
22. G. Lu, R. E. Middleton, H. Sun, M. Naniang, C. J. Ott, C. S. Mitsiades, K.-K. Wong, J. E. Bradner, W. G. Kaelin Jr., The myeloma drug lenalidomide promotes the cereblon-dependent destruction of Ikaros proteins. *Science* **343**, 305–309 (2014).
23. J. Kronke, N. D. Udeshi, A. Narla, P. Grauman, S. N. Hurst, M. McConkey, T. Svinikina, D. Heckl, E. Comer, X. Li, C. Ciardo, E. Hartman, N. Munshi, M. Schenone, S. L. Schreiber, S. A. Carr, B. L. Ebert, Lenalidomide causes selective degradation of IKZF1 and IKZF3 in multiple myeloma cells. *Science* **343**, 301–305 (2014).
24. T. Hideshima, F. Cottini, Y. Nozawa, H. S. Seo, H. Ohguchi, M. K. Samur, D. Cirstea, N. Mimura, Y. Iwasawa, P. G. Richardson, N. C. Munshi, D. Chauhan, W. Masefski, T. Utsumi, S. Dhe-Paganon, K. C. Anderson, p53-related protein kinase confers poor prognosis and represents a novel therapeutic target in multiple myeloma. *Blood* **129**, 1308–1319 (2017).
25. M. Dimopoulos, A. Spencer, M. Attal, H. M. Prince, J. L. Harousseau, A. Dmoszynska, J. San Miguel, A. Hellmann, T. Facon, R. Foà, A. Corso, Z. Masliak, M. Olesnyckij, Z. Yu, J. Patin, J. B. Zeldis, R. D. Knight; Multiple Myeloma (010) Study Investigators, Lenalidomide plus dexamethasone for relapsed or refractory multiple myeloma. *N. Engl. J. Med.* **357**, 2123–2132 (2007).
26. T. Facon, S. Kumar, T. Plesner, R. Z. Orlowski, P. Moreau, N. Bahlis, S. Basu, H. Nahi, C. Hulin, H. Quach, H. Goldschmidt, M. O'Dwyer, A. Perrot, C. P. Venner, K. Weisel, J. R. Mace, N. Raj, M. Attal, M. Tiab, M. Macro, L. Frenzel, X. Leleu, T. Ahmadi, C. Chiu, J. Wang, R. Van Rampelbergh, C. M. Uhlar, R. Kobos, M. Qi, S. Z. Usmani; MAIA Trial Investigators, Daratumumab plus lenalidomide and dexamethasone for untreated myeloma. *N. Engl. J. Med.* **380**, 2104–2115 (2019).
27. D. Heintel, A. Rocci, H. Ludwig, A. Bolomsky, S. Caltagirone, M. Schreder, S. Pfeifer, H. Gisslinger, N. Zojer, U. Jager, A. Palumbo, High expression of cereblon (CRBN) is associated with improved clinical response in patients with multiple myeloma treated with lenalidomide and dexamethasone. *Br. J. Haematol.* **161**, 695–700 (2013).
28. A. Broyl, R. Kuiper, M. van Duin, B. van der Holt, L. el Jarari, U. Bertsch, S. Zweegman, A. Buijs, D. Hose, H. M. Lokhorst, H. Goldschmidt, P. Sonneveld; Dutch-Belgian HOVON group; German GMMG Group, High cereblon expression is associated with better survival in patients with newly diagnosed multiple myeloma treated with thalidomide maintenance. *Blood* **121**, 624–627 (2013).
29. Y. X. Zhu, E. Braggio, C. X. Shi, K. M. Kortuem, L. A. Bruins, J. E. Schmidt, X. B. Chang, P. Langlais, M. Luo, P. Jedlowski, B. LaPlant, K. Laumann, R. Fonseca, P. L. Bergsagel, J. Mikhael, M. Lacy, M. D. Champion, A. K. Stewart, Identification of cereblon-binding proteins and relationship with response and survival after IMiDs in multiple myeloma. *Blood* **124**, 536–545 (2014).
30. Q. L. Sievers, J. A. Gasser, G. S. Cowley, E. S. Fischer, B. L. Ebert, Genome-wide screen identifies cullin-RING ligase machinery required for lenalidomide-dependent CRL4^{CRBN} activity. *Blood* **132**, 1293–1303 (2018).

31. J. Liu, T. Song, W. Zhou, L. Xing, S. Wang, M. Ho, Z. Peng, Y. T. Tai, T. Hideshima, K. C. Anderson, Y. Cang, A genome-scale CRISPR-Cas9 screening in myeloma cells identifies regulators of immunomodulatory drug sensitivity. *Leukemia* **33**, 171–180 (2019).
32. L. E. Franssen, I. S. Nijhof, S. Couto, M. D. Levin, G. M. J. Bos, A. Broijl, S. K. Klein, Y. Ren, M. Wang, H. R. Koene, A. C. Bloem, A. Beeker, L. M. Faber, E. van der Spek, R. Raymakers, R. J. Leguit, P. Sonneveld, S. Zweegman, H. Lokhorst, T. Mutis, A. Thakurta, X. Qian, N. W. C. J. van de Donk, Cereblon loss and up-regulation of c-Myc are associated with lenalidomide resistance in multiple myeloma patients. *Haematologica* **103**, e368–e371 (2018).
33. K. M. Kortum, E. K. Mai, N. H. Hanafiah, C. X. Shi, Y. X. Zhu, L. Bruins, S. Barrio, P. Jedlowski, M. Merz, J. Xu, R. A. Stewart, M. Andrusis, A. Jauch, J. Hillengass, H. Goldschmidt, P. L. Bergsagel, E. Braggio, A. K. Stewart, M. S. Raab, Targeted sequencing of refractory myeloma reveals a high incidence of mutations in CRBN and Ras pathway genes. *Blood* **128**, 1226–1233 (2016).
34. Y. X. Zhu, C. X. Shi, L. A. Bruins, X. Wang, D. L. Riggs, B. Porter, J. M. Ahmann, C. B. de Campos, E. Braggio, P. L. Bergsagel, A. K. Stewart, Identification of lenalidomide resistance pathways in myeloma and targeted resensitization using cereblon replacement, inhibition of STAT3 or targeting of IRF4. *Blood Cancer J.* **9**, 19 (2019).
35. J. S. Damiano, A. E. Cress, L. A. Hazlehurst, A. A. Shtil, W. S. Dalton, Cell adhesion mediated drug resistance (CAM-DR): Role of integrins and resistance to apoptosis in human myeloma cell lines. *Blood* **93**, 1658–1667 (1999).
36. Y. T. Tai, X. F. Li, I. Breitkreutz, W. Song, P. Neri, L. Catley, K. Podar, T. Hideshima, D. Chauhan, N. Raju, R. Schlossman, P. Richardson, N. C. Munshi, K. C. Anderson, Role of B-cell-activating factor in adhesion and growth of human multiple myeloma cells in the bone marrow microenvironment. *Cancer Res.* **66**, 6675–6682 (2006).
37. T. Hideshima, C. Mitsiades, G. Tonon, P. G. Richardson, K. C. Anderson, Understanding multiple myeloma pathogenesis in the bone marrow to identify new therapeutic targets. *Nat. Rev. Cancer* **7**, 585–598 (2007).
38. N. E. Sanjana, O. Shalem, F. Zhang, Improved vectors and genome-wide libraries for CRISPR screening. *Nat. Methods* **11**, 783–784 (2014).
39. J.-H. Shi, S.-C. Sun, Tumor necrosis factor receptor-associated factor regulation of nuclear factor κ B and mitogen-activated protein kinase pathways. *Front. Immunol.* **9**, 1849 (2018).
40. T. C. Yeh, V. Marsh, B. A. Bernat, J. Ballard, H. Colwell, R. J. Evans, J. Parry, D. Smith, B. J. Brandhuber, S. Gross, A. Marlow, B. Hurley, J. Lyssikatos, P. A. Lee, J. D. Winkler, K. Koch, E. Wallace, Biological characterization of ARRY-142886 (AZD6244), a potent, highly selective mitogen-activated protein kinase kinase 1/2 inhibitor. *Clin. Cancer Res.* **13**, 1576–1583 (2007).
41. S. Manier, A. Sacco, X. Leleu, I. M. Ghobrial, A. M. Roccaro, Bone marrow microenvironment in multiple myeloma progression. *J. Biomed. Biotechnol.* **2012**, 157496 (2012).
42. X. Li, Y. Yang, J. D. Ashwell, TNF-R1I and c-IAP1 mediate ubiquitination and degradation of TRAF2. *Nature* **416**, 345–347 (2002).
43. G. Barbin, M. P. Roisin, B. Zalc, Tumor necrosis factor alpha activates the phosphorylation of ERK, SAPK/JNK, and P38 kinase in primary cultures of neurons. *Neurochem. Res.* **26**, 107–112 (2001).
44. T. Hideshima, N. Nakamura, D. Chauhan, K. C. Anderson, Biologic sequelae of interleukin-6 induced PI3-K/Akt signaling in multiple myeloma. *Oncogene* **20**, 5991–6000 (2001).
45. M. Attal, V. Lauwers-Cances, G. Marit, D. Caillot, P. Moreau, T. Facon, A. M. Stoppa, C. Hulin, L. Benboubker, L. Garderet, O. Decaux, S. Leyvraz, M.-C. Vekemans, L. Voillot, M. Michallet, B. Pegourie, C. Dumontet, M. Roussel, X. Leleu, C. Mathiot, C. Payen, H. Avet-Loiseau, J.-L. Harousseau; IFM Investigators, Lenalidomide maintenance after stem-cell transplantation for multiple myeloma. *N. Engl. J. Med.* **366**, 1782–1791 (2012).
46. M. A. Dimopoulos, A. Oriol, H. Nahi, J. San-Miguel, N. J. Bahlis, S. Z. Usmani, N. Rabin, R. Z. Orlowski, M. Komarnicki, K. Suzuki, T. Plesner, S. S. Yoon, D. Ben Yehuda, P. G. Richardson, H. Goldschmidt, D. Reece, S. Lisby, N. Z. Khokhar, L. O'Rourke, C. Chiu, X. Qin, M. Guckert, T. Ahmadi, P. Moreau; POLLUX Investigators, Daratumumab, lenalidomide, and dexamethasone for multiple myeloma. *N. Engl. J. Med.* **375**, 1319–1331 (2016).
47. D. W. Rasco, K. P. Papadopoulos, M. Pourdehnad, A. K. Gandhi, P. R. Hagner, Y. Li, X. Wei, R. Chopra, K. Hege, J. DiMartino, K. Shih, A first-in-human study of novel cereblon modulator avadomide (CC-122) in advanced malignancies. *Clin. Cancer Res.* **25**, 90–98 (2019).
48. C. C. Bjorklund, J. Kang, M. Amatangelo, A. Polonskaia, M. Katz, H. Chiu, S. Couto, M. Wang, Y. Ren, M. Ortiz, F. Towfic, J. E. Flynt, W. Pierceall, A. Thakurta, Iberdomide (CC-220) is a potent cereblon E3 ligase modulator with antitumor and immunostimulatory activities in lenalidomide- and pomalidomide-resistant multiple myeloma cells with dysregulated CRBN. *Leukemia* **34**, 1197–1201 (2020).
49. M. E. Matyskiela, G. Lu, T. Ito, B. Pagarigan, C.-C. Lu, K. Miller, W. Fang, N.-Y. Wang, D. Nguyen, J. Houston, G. Carmel, T. Tran, M. Riley, L. Nosaka, G. C. Lander, S. Gaidarova, S. Xu, A. L. Ruchelman, H. Handa, J. Carmichael, T. O. Daniel, B. E. Cathers, A. Lopez-Girona, P. P. Chamberlain, A novel cereblon modulator recruits GSPT1 to the CRL4^{CRBN} ubiquitin ligase. *Nature* **535**, 252–257 (2016).
50. K. Dimopoulos, H. Fibiger Munch-Petersen, C. Winther Eskelund, L. Dissing Sjo, E. Ralfkiaer, P. Gimsing, K. Gronbaek, Expression of CRBN, IKZF1, and IKZF3 does not predict lenalidomide sensitivity and mutations in the cereblon pathway are infrequent in multiple myeloma. *Leuk. Lymphoma* **60**, 180–188 (2019).
51. P. A. Huang, S. L. Beedie, C. H. Chau, D. J. Venzon, S. Gere, D. Kazandjian, N. Korde, S. Mailankody, O. Landgren, W. D. Figg, Cereblon gene variants and clinical outcome in multiple myeloma patients treated with lenalidomide. *Sci. Rep.* **9**, 14884 (2019).
52. A. J. Wood, T. W. Lo, B. Zeitler, C. S. Pickle, E. J. Ralston, A. H. Lee, R. Amora, J. C. Miller, E. Leung, X. Meng, L. Zhang, E. J. Rebar, P. D. Gregory, F. D. Urnov, B. J. Meyer, Targeted genome editing across species using ZFNs and TALENs. *Science* **333**, 307 (2011).
53. L. Cong, F. A. Ran, D. Cox, S. Lin, R. Barretto, N. Habib, P. D. Hsu, X. Wu, W. Jiang, L. A. Marraffini, F. Zhang, Multiplex genome engineering using CRISPR/Cas systems. *Science* **339**, 819–823 (2013).
54. Y. Zhou, S. Zhu, C. Cai, P. Yuan, C. Li, Y. Huang, W. Wei, High-throughput screening of a CRISPR/Cas9 library for functional genomics in human cells. *Nature* **509**, 487–491 (2014).
55. O. Shalem, N. E. Sanjana, F. Zhang, High-throughput functional genomics using CRISPR-Cas9. *Nat. Rev. Genet.* **16**, 299–311 (2015).
56. T. Hideshima, D. Chauhan, P. Richardson, C. Mitsiades, N. Mitsiades, T. Hayashi, N. Munshi, L. Dang, A. Castro, V. Palombella, J. Adams, K. C. Anderson, NF- κ B as a therapeutic target in multiple myeloma. *J. Biol. Chem.* **277**, 16639–16647 (2002).
57. A. L. Shaffer, N. C. T. Emre, L. Lamy, V. N. Ngo, G. Wright, W. Xiao, J. Powell, S. Dave, X. Yu, H. Zhao, Y. Zeng, B. Chen, J. Epstein, L. M. Staudt, IRF4 addiction in multiple myeloma. *Nature* **454**, 226–231 (2008).
58. G. Teoh, M. Urashima, A. Ogata, D. Chauhan, J. A. DeCaprio, S. P. Treon, R. L. Schlossman, K. C. Anderson, MDM2 protein overexpression promotes proliferation and survival of multiple myeloma cells. *Blood* **90**, 1982–1992 (1997).
59. S. Y. Lee, A. Reichlin, A. Santana, K. A. Sokol, M. C. Nussenzweig, Y. Choi, TRAF2 is essential for JNK but not NF- κ B activation and regulates lymphocyte proliferation and survival. *Immunity* **7**, 703–713 (1997).
60. M. Rothe, V. Sarma, V. M. Dixit, D. V. Goeddel, TRAF2-mediated activation of NF- κ B by TNF receptor 2 and CD40. *Science* **269**, 1424–1427 (1995).
61. S. E. Alvarez, K. B. Harikumar, N. C. Hait, J. Allegood, G. M. Strub, E. Y. Kim, M. Maceyka, H. Jiang, C. Luo, T. Kordula, S. Miltstien, S. Spiegel, Sphingosine-1-phosphate is a missing cofactor for the E3 ubiquitin ligase TRAF2. *Nature* **465**, 1084–1088 (2010).
62. J. J. Keats, R. Fonseca, M. Chesi, R. Schop, A. Baker, W. J. Chng, S. Van Wier, R. Tiedemann, C. X. Shi, M. Sebag, E. Braggio, T. Henry, Y. X. Zhu, H. Fogle, T. Price-Troska, G. Ahmann, C. Mancini, L. A. Brents, S. Kumar, P. Greipp, A. Dispenzieri, B. Bryant, G. Mulligan, L. Bruhn, M. Barrett, R. Valdez, J. Trent, A. K. Stewart, J. Carpten, P. L. Bergsagel, Promiscuous mutations activate the noncanonical NF- κ B pathway in multiple myeloma. *Cancer Cell* **12**, 131–144 (2007).
63. D. Chauhan, S. Kharbanda, A. Ogata, M. Urashima, G. Teoh, M. Robertson, D. W. Kufe, K. C. Anderson, Interleukin-6 inhibits Fas-induced apoptosis and stress-activated protein kinase activation in multiple myeloma cells. *Blood* **89**, 227–234 (1997).
64. O. Sezer, C. Jakob, J. Eucker, K. Niemöller, F. Gatz, K. Wernecke, K. Possinger, Serum levels of the angiogenic cytokines basic fibroblast growth factor (bFGF), vascular endothelial growth factor (VEGF) and hepatocyte growth factor (HGF) in multiple myeloma. *Eur. J. Haematol.* **66**, 83–88 (2001).
65. T. Hideshima, D. Chauhan, R. Schlossman, P. Richardson, K. C. Anderson, The role of tumor necrosis factor α in the pathophysiology of human multiple myeloma: Therapeutic applications. *Oncogene* **20**, 4519–4527 (2001).

Acknowledgments: We thank E. Campeau, M. Robinson, and F. Zhang for expression vectors. We also thank D. Chauhan and E. Morelli for helpful comments. We thank the staff from the hematologic neoplasia core facilities at DFCI for technical assistance. We also thank the Genome Center of WuXi AppTec Inc. for the initial data analysis of the CRISPR screening. **Funding:** This work was supported by the National Institutes of Health grants SPORE-P50100707 (to K.C.A.), R01-CA050947 (to K.C.A.), R01-CA178264 (to T.H. and K.C.A.), and P01-155258 (K.C.A. and N.M.). K.C.A. is an American Cancer Society Clinical Research Professor. This study was also supported, in part, by the Dr. Miriam and Sheldon G. Adelson Medical

Research Foundation, the Riney Family Myeloma Initiative, and the National Natural Science Foundation of China (NSFC grant no. 81800204). **Author contributions:** K.C.A. conceived the project, designed the research, analyzed the data, wrote the manuscript, and supervised the project. J.L. and T.H. designed and performed the research, analyzed data, and wrote the manuscript. J.L. and L.X. performed xenograft experiments. S.W. and W.Z. performed CRISPR-Cas9 screening data analysis. M.K.S. analyzed RNA-seq data from patients with MM. T.S. performed immunohistochemistry. D.O. provided assistance in some cell-based assays. G.A. and G.B. provided BM sections. S.G. and L.Y. performed immunohistochemistry. T.J. performed some Western blot experiments. K.W. helped process the human samples. R.C. provided biological materials and performed immunohistochemistry. Y.-T.T. provided biological material and analyzed data. N.M. and P.R. helped collect patient samples and analyzed data. Y.C. helped analyze data and revised the manuscript. **Competing interests:** K.C.A. serves on advisory boards to Millennium, Janssen, Sanofi, Bristol Myers Squibb, Gilead, Precision Biosciences, and Tolero and is a scientific founder of OncoPep and C4 Therapeutics. The

authors declare that they have no other competing interests. **Data and materials availability:** All data needed to evaluate the conclusions in the paper are present in the paper and/or the Supplementary Materials. All sequencing data were uploaded to Gene Expression Omnibus with accession no. GSE171341.

Submitted 21 December 2020

Accepted 19 April 2021

Published 4 June 2021

10.1126/sciadv.abg2697

Citation: J. Liu, T. Hideshima, L. Xing, S. Wang, W. Zhou, M. K. Samur, T. Sewastianik, D. Ogiya, G. An, S. Gao, L. Yang, T. Ji, G. Bianchi, K. Wen, Y.-T. Tai, N. Munshi, P. Richardson, R. Carrasco, Y. Cang, K. C. Anderson, ERK signaling mediates resistance to immunomodulatory drugs in the bone marrow microenvironment. *Sci. Adv.* **7**, eabg2697 (2021).

ERK signaling mediates resistance to immunomodulatory drugs in the bone marrow microenvironment

Jiye Liu, Teru Hideshima, Lijie Xing, Su Wang, Wenrong Zhou, Mehmet K. Samur, Tomasz Sewastianik, Daisuke Ogiya, Gang An, Shaobing Gao, Li Yang, Tong Ji, Giada Bianchi, Kenneth Wen, Yu-Tzu Tai, Nikhil Munshi, Paul Richardson, Ruben Carrasco, Yong Cang and Kenneth C. Anderson

Sci Adv 7 (23), eabg2697.
DOI: 10.1126/sciadv.abg2697

ARTICLE TOOLS

<http://advances.sciencemag.org/content/7/23/eabg2697>

SUPPLEMENTARY MATERIALS

<http://advances.sciencemag.org/content/suppl/2021/05/28/7.23.eabg2697.DC1>

REFERENCES

This article cites 65 articles, 27 of which you can access for free
<http://advances.sciencemag.org/content/7/23/eabg2697#BIBL>

PERMISSIONS

<http://www.sciencemag.org/help/reprints-and-permissions>

Use of this article is subject to the [Terms of Service](#)

Science Advances (ISSN 2375-2548) is published by the American Association for the Advancement of Science, 1200 New York Avenue NW, Washington, DC 20005. The title *Science Advances* is a registered trademark of AAAS.

Copyright © 2021 The Authors, some rights reserved; exclusive licensee American Association for the Advancement of Science. No claim to original U.S. Government Works. Distributed under a Creative Commons Attribution NonCommercial License 4.0 (CC BY-NC).